Constraints on dolomite formation in a Late Palaeozoic saline alkaline lake deposit, Junggar Basin, north-west China

Guo, Pei; Wen, Huaguo; Sánchez-Román, Mónica

published in
Sedimentology
2023

DOI (link to publisher)
10.1111/sed.13122

document version
Publisher's PDF, also known as Version of record

SEDIMENTOLOGY the journal of the International Association of Sedimentologists

Sedimentology (2023) **70**, 2302–2330 doi: 10.1111/sed.13122

Constraints on dolomite formation in a Late Palaeozoic saline alkaline lake deposit, Junggar Basin, north-west China

PEI GUO* , HUAGUO WEN* and MÓNICA SÁNCHEZ-ROMÁN†
**State Key Laboratory of Oil and Gas Reservoir Geology and Exploitation, Institute of Sedimentary Geology, Chengdu University of Technology, Chengdu, Sichuan 610059, China (E-mail: wenhuaguo08@cdut.cn)*
†Earth Sciences Department, Vrije Universiteit Amsterdam, de Boelelaan 1085, Amsterdam 1081 HV, The Netherlands

Associate Editor – Hilary Corlett

ABSTRACT

Alkaline lakes (pH > 9) are among the few modern sedimentary environments that are hydrochemically favourable for low-temperature dolomite formation. While Mg-clays and Mg-evaporites also form more easily in alkaline environments, few studies have focused on how the kinetically inhibited dolomite wins the competition for Mg^{2+}. Here, a basin-wide survey of the distribution, paragenesis and stable C, O and Mg isotopes of main Mg-rich minerals in the Late Palaeozoic saline alkaline lake deposit of the north-west Junggar Basin, north-west China, is conducted to study the influence of the formation and diagenesis of eitelite, northupite and Mg-clays on dolomite formation. Large, isolated dolomite crystals (20 to 70 μm in diameter), show positive $\delta^{13}C$ values (ranging from +1 to +7‰) and a restricted distribution in the mudstones of the lake-transitional zone. These crystals have been interpreted as organogenic dolomite driven by methanogenesis via fermentation of organic substrates. The $\delta^{18}O$ values of dolomitic mudstones (from −7.4 to +3.4‰), calcitic mudstones (from −15.1 to −3.3‰) and bedded Na-carbonate evaporites (from +0.08 to +3.7‰), together with their Mg isotopic compositions, suggest that dolomite was not enriched in the most concentrated environments or during stages with most Mg sources, but in the organic-rich deposits containing few other authigenic Mg-rich minerals. Dolomite is at a competitive disadvantage for Mg^{2+} ions compared to Mg-evaporite and Mg-clay minerals due to its slow crystallization rates and the deficiency of micritic calcium carbonate precursors. However, it can nucleate and progressively grow into large crystals (>20 μm) if bacterial methanogenesis could effectively lower porewater pH (<8.5) and induce the dissolution of generated eitelite, northupite or Mg-clays. These findings suggest that high salinity and/or high alkalinity are not always favourable conditions for dolomite formation and highlight the active role of pH fluctuations in inducing low-temperature dolomite formation.

Keywords Methanogenesis, Mg-rich clays, Mg-rich evaporites, organogenic dolomite, pH fluctuation, stable Mg isotopes.

INTRODUCTION

Alkaline (pH > 9) lakes are among the few modern sedimentary environments where disordered dolomite primarily precipitates under Earth's surface conditions (Smith & Stuiver, 1979; Wright & Wacey, 2005; Meister *et al.*, 2011; Last *et al.*, 2012; McCormack *et al.*, 2018; Fussmann *et al.*, 2020; del Buey & Sanz-Montero, 2022). Many ancient dolomite-rich lacustrine deposits

were developed in alkaline lake systems (Southgate *et al.*, 1989; Calvo *et al.*, 1995; Bowen *et al.*, 2008; Casado *et al.*, 2014; Murphy *et al.*, 2014; Yao *et al.*, 2017; Cao *et al.*, 2020). The Precambrian massive deposits of dolomite might be related to low-temperature (T) formation processes in alkaline oceans (Kempe & Degens, 1985; Meister *et al.*, 2011; Meister, 2013). The formation of low-T dolomite in alkaline environments can be attributed to the following three physico-chemical conditions.

1 In alkaline environments there are abundant inorganic catalysts to enhance the desolvation of Mg^{2+}–H_2O complexes and promote the formation of metastable Ca-Mg-carbonates. For example, dissolved silica (SiO_2), which is very abundant in alkaline solutions due to its solubility positively being correlated with water pH, has been suggested as a very effective catalyst for dolomite formation (Hobbs & Xu, 2020; Fang & Xu, 2022; Fang *et al.*, 2023). Sulphate in alkaline lakes will be quickly reduced to dissolved hydrogen sulphide, the latter of which can adsorb onto the surface of Mg^{2+}–H_2O complexes and increase the Mg^{2+}-H_2O distance, weakening the bonding of Mg^{2+}-H_2O (Zhang *et al.*, 2012; Shen *et al.*, 2014).

2 In addition to dehydration of Mg^{2+}–H_2O complexes in alkaline solutions, the vast quantity of dissolved inorganic carbon will produce high degrees of supersaturation with respect to dolomite, if the saturation with respect to Mg-silicates has not been reached (Chase *et al.*, 2021). Although low-T dolomite formation is kinetically inhibited, not thermodynamically unfavoured, many studies have claimed that ordered dolomite can form via non-classical crystallization processes involving nucleation and aggregation (Meister & Frisia, 2019; Raudsepp *et al.*, 2022). Such precursor phases include amorphous Ca-Mg carbonates, crystalline nano-particles composed of metastable Ca-Mg-carbonates with different Mg/Ca ratios (high Mg-calcite, protodolomite, non-ordered Ca-rich dolomite), which require much lower bulk free energies and form more easily in natural environments than ordered dolomite.

3 The high carbonate alkalinity of alkaline lakes can effectively buffer the decreased pH that results from microbial respiration reactions, most re-oxidation reactions, mineralization processes of organic matter by sulphate reduction, methanogenesis and anaerobic methane oxidation (Soetaert *et al.*, 2007), and protect primary carbonate precipitates from dissolution (Meister, 2013).

On the other hand, dolomite is rarely found in many modern alkaline lakes such as the: (i) lakes in the East Africa Valley (Last, 1990), which are rich in Mg-Na-evaporites [tychite ($2MgCO_3{\cdot}2Na_2CO_3{\cdot}Na_2SO_4$); northupite, $Na_2CO_3{\cdot}MgCO_3{\cdot}NaCl$] (Arad & Morton, 1969; Kilham & Melack, 1972); (ii) Lake Salda in south-east Turkey, rich in nesquehonite ($MgCO_3{\cdot}3H_2O$), dypingite [$Mg_5(CO_3)_4(OH)_2{\cdot}5H_2O$] and hydromagnesite [$Mg_5(CO_3)_4(OH)_2{\cdot}4H_2O$] (Shirokova *et al.*, 2011); and (iii) lakes in British Columbia, rich in hydromagnesite and magnesite ($MgCO_3$) (Power *et al.*, 2019). The early Cretaceous highly alkaline lakes within South Atlantic rift–sag lacustrine basins are also rich in authigenic Mg-clays [stevensite $(Na,Ca)_{0.3}Mg_3Si_4O_{10}(OH)_2{\cdot}nH_2O$] instead of primary dolomite (Tosca & Wright, 2015; Wright & Barnett, 2015; Mercedes-Martín *et al.*, 2019). Under similar hypersaline conditions, Mg-evaporite-bearing shales of alkaline hypersaline lakes contain statistically less dolomite (generally <50%: Boak & Poole, 2015; Guo *et al.*, 2021) than the sulphate-bearing shales of non-alkaline hypersaline lakes (easily >50%: Li *et al.*, 2018; Guo *et al.*, 2019). Apparently, the formation of dolomite in low-T alkaline environments is constrained by the authigenesis of other Mg-rich minerals, including Mg-Na-carbonate evaporites (tychite, northupite, etc.), clays (stevensite, sepiolite, etc.) or other carbonate phases (hydromagnesite). The increased Mg^{2+} ion availability in alkaline environments, resulting from various Mg^{2+} sources and lowered hydration energy of Mg^{2+} ions, will not only facilitate the formation of low-temperature dolomite, but also allow the precipitation of other Mg-rich minerals. Understanding the hydrochemical and physico-chemical conditions that control the formational precedence of different Mg-rich minerals in alkaline environments will provide valuable information about the pore evolution of hydrocarbon reservoirs (Tosca & Wright, 2015; Wright & Barnett, 2015) and help inform studies of Precambrian seawater chemistry (Kempe & Degens, 1985; Meister, 2013).

The influence of the authigenesis of Mg-rich clays on dolomite formation and dissolution has been little studied (e.g. Bristow *et al.*, 2012; Tosca & Wright, 2015; Ryan *et al.*, 2019; Chase *et al.*, 2021). Clay minerals in alkaline lake deposits are generally Mg-bearing and commonly include Mg-rich smectites, palygorskite,

sepiolite, stevensite, etc. (Tosca & Wright, 2015; del Buey *et al.*, 2018; Pozo & Calvo, 2018; Tutolo & Tosca, 2018; Table 1). Diagenetic relationships between Mg-clays and Ca-Mg-carbonates can be classified into the following.

1 The existence of clays facilitates proto-dolomite (non-ordered Ca-rich dolomite and/or very high Mg-calcite) formation, by providing templates for dolomite nucleation or by keeping high alkalinity water in its clay structures (Díaz-Hernández *et al.*, 2013; Casado *et al.*, 2014; Liu *et al.*, 2019; Wen *et al.*, 2020).

2 At an early diagenetic stage, the formation of Mg-rich clays via transformation of reactive detrital dioctahedral smectite or from authigenesis provides a sink for Mg^{2+} in porewaters, limiting authigenic dolomite precipitation (Bristow *et al.*, 2012; Chase *et al.*, 2021).

3 Dolomite from newly deposited sediments of alkaline playa-lake environments will be dissolved due to a pH decrease in the diagenetic system, which could result from sulphide oxidation ($H_2S + 2O_2 \rightarrow SO_4^{2-} + 2H^+$) during the drying of lake waters (Leguey *et al.*, 2010) or from the infiltration of acid meteoric waters (Chahi *et al.*, 1999; Ryan *et al.*, 2019). The dissolution of dolomite not only supplied the Mg^{2+} for the Mg-clay (sepiolite, stevensite and palygorskite) formation but also buffered the pH at values required for continuous formation of Mg-clays.

4 Inversely, methanogenic anaerobic degradation of organic matter will produce organic acids and CO_2, lower porewater pH and consequently induce dissolution of Mg-clays (stevensite) in deep organic-rich sediments releasing Mg^{2+} to enhance widespread dolomitization (Tosca & Wright, 2015; Wright & Barnett, 2015). These studies suggest that Mg cycling between Mg-rich clays and carbonates is more common than expected, which can greatly influence dolomite formation and diagenesis. There are more Mg-rich evaporite precipitates in alkaline hypersaline lakes than in non-alkaline hypersaline

Table 1. Chemical formulas and relative amounts of minerals studied in the Fengcheng Formation of the Mahu Sag of the Junggar Basin.

Mineral	Mineral	Chemical formulas	Abundance*	Abbreviation
Na-carbonate	Trona	$Na_2CO_3{\cdot}NaHCO_3{\cdot}2H_2O$	II	
	Wegscheiderite	$Na_2CO_3{\cdot}3NaHCO_3$	II	
Mg-Na-carbonate	Eitelite	$Na_2CO_3{\cdot}MgCO_3$	II	Et
	Northupite	$Na_2CO_3{\cdot}MgCO_3{\cdot}NaCl$	II	Nor
	Bradleyite	$Na_3PO_4{\cdot}MgCO_3$	IV	
Ca-Na-carbonate	Gaylussite	$Na_2CO_3{\cdot}CaCO_3{\cdot}5H_2O$	V	
	Pirssonite	$Na_2CO_3{\cdot}CaCO_3{\cdot}2H_2O$	V	
	Shortite	$Na_2CO_3{\cdot}2CaCO_3$	II	St
Ca-Mg-carbonate	Dolomite	$CaCO_3{\cdot}MgCO_3$	II	Dol
	Calcite	$CaCO_3$	II	Cc
	Magnesite	$MgCO_3$	IV	Mag
	Hydromagnesite	$(Mg_5(CO_3)_4(OH)_2{\cdot}4H_2O)$	VI	
Mg-clays†	Sepiolite	$Mg_4Si_6O_{15}(OH)_2{\cdot}6H_2O$	III	Sep
	Palygorskite	$(Mg,Al)_2Si_4O_{10}(OH){\cdot}4H_2O$	VI	
	Stevensite	$(Na,Ca)_{0.3}Mg_3Si_4\ O_{10}(OH)_2{\cdot}nH_2O$	VI	
	Mg-illite	$KAl_2(Si_3Al)O_{10}(OH)_2$	I	Ms
	Clinochlore	$Mg_5Al(AlSi_3)O_{10}(OH)_8$	II	Ms
	Mg-smectite	$(Al_{1.5}Fe^{3+}{}_{0.2}Mg_{0.3})Si_4O_{10}(OH)_2]^{-0.3}{\cdot}(Ca,Na){\cdot}nH_2O$	VI	
Borosilicate	Reedmergnerite	$NaBSi_3O_8$	II	Rd
	Searlesite	$NaBSi_2O_6{\cdot}H_2O$	III	Sl
Feldspar	K-feldspar	$KAlSi_3O_8$	I	Kf
	Albite	$NaAlSi_3O_8$	I	Ab

*Classification (modified after Milton, 1971): I – ubiquitous and abundant; II – locally abundant; III – local and never abundant; IV – local and sparse; V – once abundant, now totally transformed; VI – discussed but not present in Fengcheng Formation. †EDS analyses indicate all clays in the Fengcheng Formation contain a steady Mg peak.

lakes, the former of which commonly include northupite and eitelite [$Na_2Mg(CO_3)_2$] (Table 1; Kilham & Melack, 1972; Smith & Stuiver, 1979; Mees *et al.*, 1991; Dyni, 1996; Yu *et al.*, 2018). These anhydrous Mg-Na-carbonates and their capacity to directly precipitate from lake waters (Kilham & Melack, 1972; Mees *et al.*, 1991) can prove critical for the availability of free Mg^{2+} ions in alkaline lakes and help to understand whether the strong hydration of Mg^{2+} ions is an intrinsic inhibitor for low-T dolomite formation in high-pH environments or not (Xu *et al.*, 2013; Pimentel & Pina, 2016; Zhou *et al.*, 2021).

This study focuses on the impacts of the formation and dissolution of Mg-rich minerals (eitelite, northupite and Mg-clays) on dolomite formation in alkaline lake systems. The Fengcheng Formation of the Mahu Sag in the north-west Junggar Basin, north-west China (Fig. 1A) was deposited in a Late Palaeozoic volcanic-related saline alkaline lake (Yu *et al.*, 2018, 2019; Cao *et al.*, 2020). This closed soda lake had a contrasting basement relief and was filled with laterally distinctive deposits (Yu *et al.*, 2019), from orogen proximal margin to lake centre and distal margin, including volcanoclastic conglomerates, sandstones, Na-carbonate evaporites, dolomitic mudstones and calcitic mudstones (Yu *et al.*, 2018, 2019; Guo *et al.*, 2021). Many hydrocarbon exploration boreholes have been drilled in the Fengcheng Formation (Fig. 1B) and subsequently examined; therefore it is an ideal setting to study the formation of Mg-rich minerals like Mg-evaporites (eitelite and northupite), dolomite and Mg-clays (Mg-illite, sepiolite and clinochlore) under different physico-chemical conditions (pH, Mg/Ca and salinity). In this study, through examination of the basin-wide survey, the distribution of major Mg-rich minerals in different geographical locations is determined. Based on the paragenesis of Mg-rich minerals and stable C, O and Mg isotopes, the Mg^{2+} sources, and main Mg sinking and fixing processes in the central, transitional and marginal zones of alkaline lakes are reconstructed. Finally, the restricting and driving factors for dolomite formation in alkaline environments are proposed.

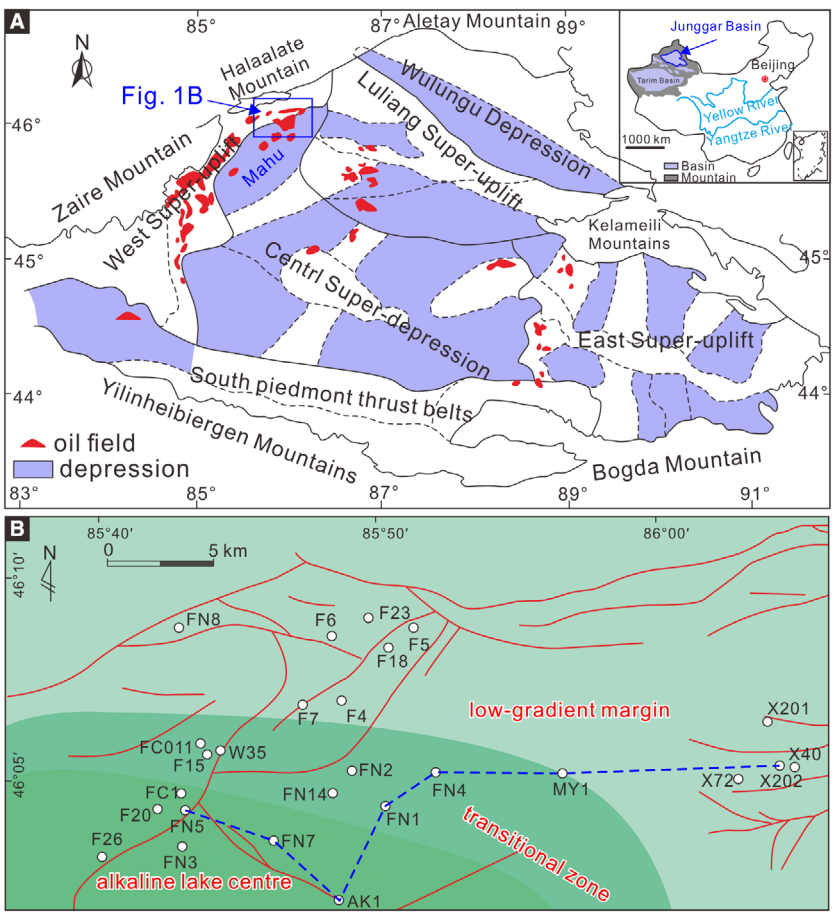

Fig. 1. (A) Location of the Junggar Basin and the studied Mahu Sag. (B) Distribution of important wells (white dots) of the Fengcheng Formation in the Mahu Sag.

GEOLOGICAL SETTING AND LITHOSTRATIGRAPHY

The Junggar Basin has an area of 1.3×10^5 km^2 and is the second largest sedimentary basin in north-west China (Fig. 1A), after the Tarim Basin to the south. The Junggar Basin formed during the Late Carboniferous to Early Permian when the lithosphere of the trapped Junggar Ocean within the Kazakhstan orocline on the north-east Pangea subducted and collided with the Tarim Plate to the south and the Siberian Plate to the north (Carroll *et al.*, 1990). A >2 km thick shoaling-upward volcano-marine succession recorded the retreat of marine waters from the southern Junggar Basin during this period (Carroll *et al.*, 1990), and is overlain by Permian nonmarine strata with a total thickness of over 4 km.

The petroleum-rich Mahu Sag is in the north-west Junggar Basin (Fig. 1A), and lacustrine deposition began earlier here than in the south part of the basin. The Late Carboniferous Jiamuhe Formation was the first lacustrine sequence deposited in the Mahu Sag and is characterized by a mixture of lacustrine clastic–carbonate rocks and volcanic rocks. The overlying Fengcheng Formation (*ca* 300 Ma) contains fewer volcanic rocks than the Jiamuhe Formation and is dominated by lacustrine Na-carbonate evaporites, carbonates, siliciclastics and tuffs, which represent deposition in a closed volcanic-related saline alkaline lake. This soda lake was developed in an asymmetrical isolated sag with a proximal steep margin in the south-west and several wide low-gradient margins located in the north-east, east, south-east and southern parts (Fig. 2; Yu *et al.*, 2019). The present study area, Urho–Xiazijie (Fig. 1B), is divided into three tectono-sedimentary zones: (i) lake centre; (ii) transitional zone; and (iii) wide low-gradient margin (Fig. 2).

The Fengcheng Formation is subdivided into three members, which correspond to the three stages of lake evolution (Fig. 2) as a response to the brine chemistry changes of an endorheic lake settled in volcanogenic terrains fed by mixing fresh and hydrothermal waters. The first member (FC1) inherited the sedimentary and volcanic setting of the underlying Jiamuhe Formation and contains a large proportion of volcaniclastic rocks, vesicular rhyolitic ignimbrites and alluvial-fan volcanoclastic conglomerate near the volcanoes (Fig. 2). The FC1 lake was a volcanic alkaline lake. During deposition of the second member (FC2), volcanic activity weakened and mainly occurred in the south-western deep margin of the Mahu Sag. Abundant Na-carbonate evaporites have been drilled and cored in lake centre deposits and correspond to the most saline stage of the lake (Yu *et al.*, 2019). The FC2 lake was a saline alkaline lake. When the third member (FC3) was deposited, volcanic activity was further reduced, water salinity of the lake was largely lowered, and the input of terrestrial clay and silt grains was gradually increased. The FC3 lake was an alkaline playa-lake (Fig. 2).

METHODS

Core logging and sample collection were carried out at the Xinjiang Oil Field Company, north-west China. A total of 200 thin sections were cut normal to the primary bedding of the rocks and stained with Alizarin Red-S. The different mineral phases present in the Fengcheng Formation were first observed and identified using a polarized light microscope (Nikon LV100POL, Tokyo, Japan). Thin sections with complicated mineralogical associations were scanned by an HP scanner (M1005 MFP, Hewlett Packard, Palo Alto, CA, USA). Their pictures were marked with different colours to show the distribution of different mineral phases. Paragenetic sequences were reconstructed by using an FEI Quanta-200 environmental scanning electron microscope (ESEM; FEI Company, Hillsboro, OR, USA) coupled with a backscattered electron detector (BSED) and an EDAX-Genesis X-ray energy dispersive spectrometer (EDS; EDAX Inc., Pleasanton, CA, USA) at the Scientific and Technological Centers, University of Barcelona (CCiTUB). Samples with abundant unknown minerals that could not be determined by thin sections or EDS testing were further analysed by X-ray diffraction (XRD). The XRD patterns of the most significant studied rocks are presented in Fig. 3 to show the typical mineralogy of the lake deposits. Dolomite-rich samples were specifically analysed in thin sections using fluorescence microscopy (NikonL V100POL-FL) and cathodoluminescence microscopy (CL8200 MK5-2; CITL, Cambridge, UK, under operating conditions of 300 mA and 17 kV) at the State Key Laboratory of Oil and Gas Reservoir Geology and Exploitation, Chengdu University of Technology, China.

After mineralogical analysis, 48 samples containing different carbonate minerals (including Na-carbonate evaporites) were selected for stable isotopic analysis of carbon (C) and oxygen

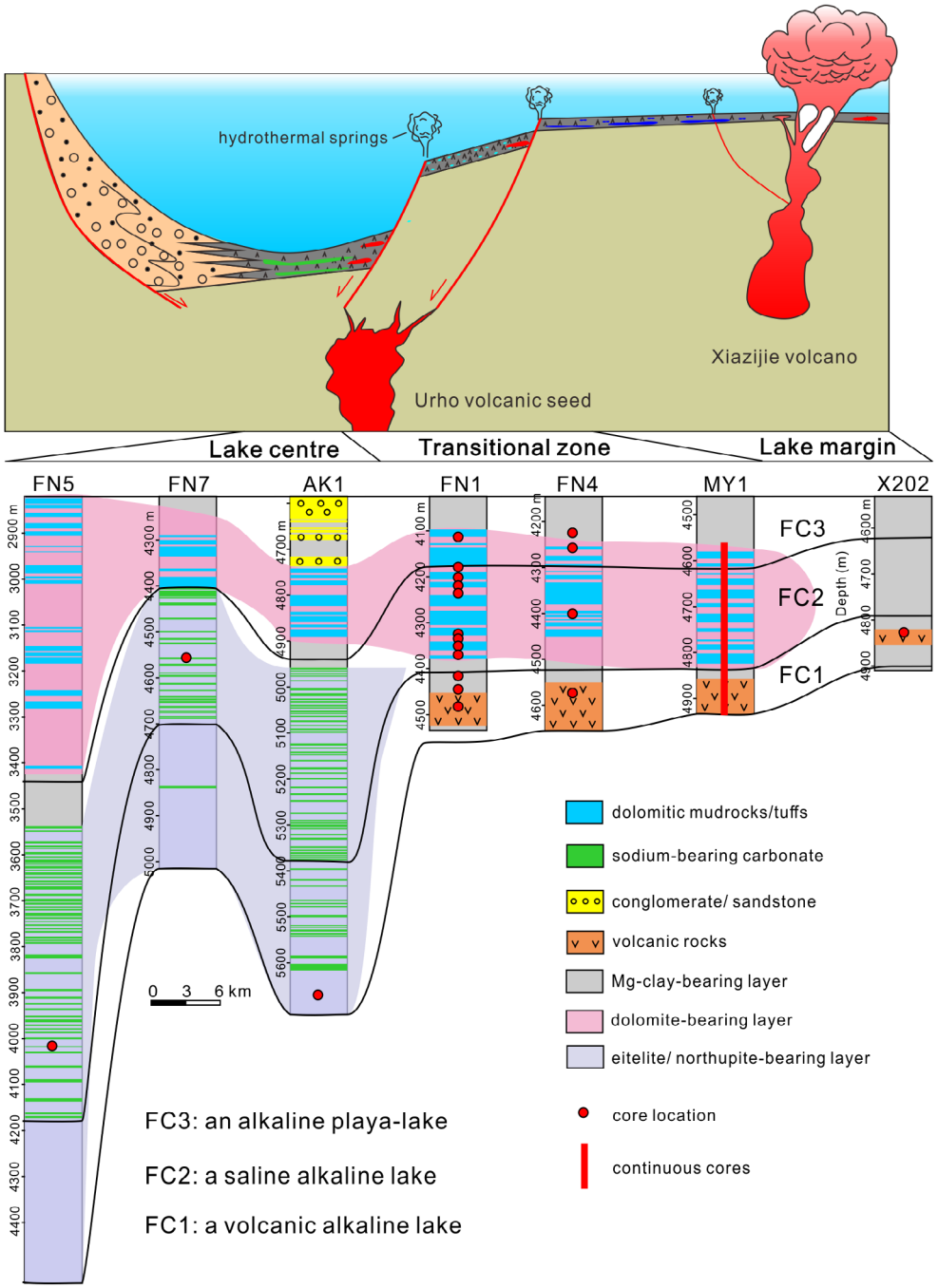

Fig. 2. A cross-facies profile showing the lateral and stratigraphic distribution of major Mg-bearing minerals. See Fig. 1B for profile location and Figs 3 to 8 for further detailed petrology and mineralogy.

(O; Table S1), at the Laboratory for Stable Isotope Geochemistry, Institute of Geology and Geophysics, Beijing, China. Each 500 μg sample was directly reacted with H_3PO_4 (100%) at 70°C. The released CO_2 was collected, cryogenically purified, and C and O isotopes were measured using a MAT253, mass spectrometer (Thermo Finnigan MAT GmbH, Bremen, Germany). The accuracy and precision were routinely checked by running a carbonate standard [IVA-CO-1 ($\delta^{13}C_{VPDB}$ = +2.21‰, $\delta^{18}O_{VPDB}$ = +1.90‰)] after every sixth sample measurement, and the values were measured relative to the international standard NBS 19. Analytical reproducibility is better

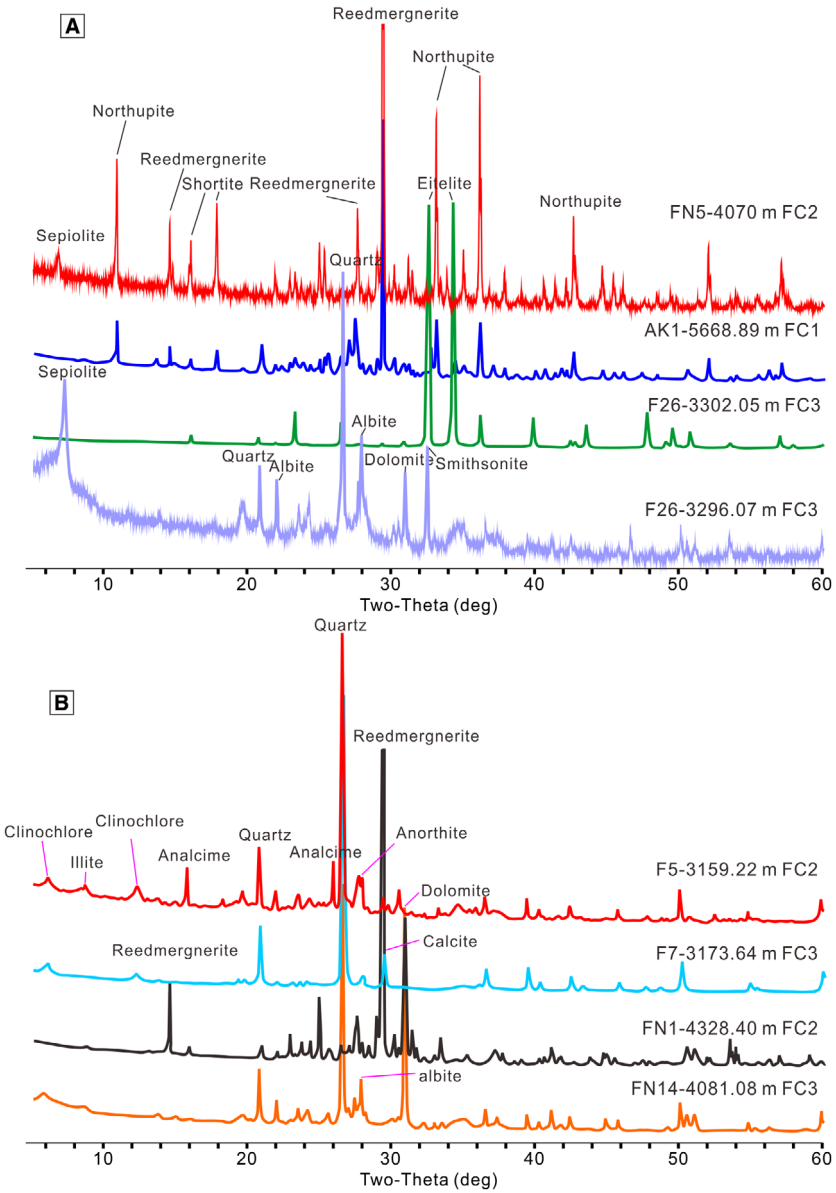

Fig. 3. X-ray diffraction (XRD) patterns of typical rocks collected from different depositional zones of the Late Palaeozoic alkaline lake in the Mahu Sag. (A) XRD patterns showing the mineral compositions of lake-central deposits; (B) XRD patterns showing the mineral compositions of lake-transitional (FN1 and FN14) and lake-marginal (F5 and F7) deposits.

than 0.15‰ for $\delta^{13}C$ and better than 0.20‰ for $\delta^{18}O$. Carbonate isotopic results are reported using standard δ (per mil, ‰) notation relative to the Vienna Pee Dee Belemnite standard (VPDB).

Eighteen samples of different Mg-rich minerals were also selected for Mg isotope analysis (Table S2). Centimetre-sized eitelite crystals were specially collected by a micro-drilling tool. Powders of the 18 samples were sent for Mg purification and mass spectrometry analyses to the State Key Laboratory of Continental Dynamics (SKLCD), Department of Geology, Northwest University, China. Magnesium isotopic ratios were measured using a Nu Plasma II MC-ICPMS (Nu Instruments, Wrexham, UK) at the SKLCD. The Nu Plasma II is a double-focusing mass spectrometer with 16 Faraday cups and five full-size discrete dynode multipliers. The in-house Mg solution GSB-Mg was analysed during each analytical session to assess data quality and to determine the long-term reproducibility of Mg isotopic ratios measurements. Details for chemical processes of Mg purification and testing processes of mass spectrometry are in Bao *et al.* (2019).

RESULTS

Magnesium-rich minerals of the saline alkaline lake-central zone

The dominant Mg-rich minerals in lake-central deposits of the two saline alkaline lake stages (FC1 and FC2) are eitelite and northupite (Figs 3A and 4; Table S2), whereas dolomite is almost absent in the Mg-evaporite-rich beds (Fig. 3A) and Mg-clays like Mg-illite and sepiolite are present, but in negligible amounts. Laminated (<1 cm) and bedded Na-carbonate evaporites occur in the lake-central deposits of FC1 and FC2 and are comparatively more abundant in the more saline stage FC2 (Table 1). However, FC2 mainly contains thinly to thickly bedded grass-like Na-carbonate evaporites (trona and wegscheiderite; Table 1; Yu *et al.*, 2018), while FC1 mainly consists of laminated to thinly bedded eitelite and northupite, reflecting the different water chemistry of the two stages. Between Na-carbonate evaporite beds are mudstone intervals that also contain abundant euhedral evaporite crystals or nodules.

A typical thinly-bedded (1 to 10 cm thick) sample of FC1 (Fig. 4A) was selected to study the origin and paragenesis of Mg-evaporites, which consists of six layers that are quite distinct in their mineral composition. From lower to upper, this sample includes: (1) northupite-cemented mudstone; (2) northupite-dominant evaporite; (3) northupite-cemented mudstone; (4) mudstone; (5) eitelite-dominant evaporite; and (6) laminated mudstone. Among the six layers, the northupite layer (2) is the most complex in terms of mineral composition, consisting of northupite, shortite, eitelite and reedmergnerite (Fig. 4A). The BSE and photomicrographs show the subsequent replacement of eitelite by northupite, shortite and reedmergnerite (Fig. 4B and C) and prove that the original eitelite has been intensively replaced by northupite. Comparatively, the eitelite layer (5) is relatively simpler in mineral composition, with only euhedral reedmergnerite crystals dispersed in an eitelite substrate. The mudstone layers (4) and (6) are mainly composed of mosaic irregular albite and K-feldspar, as well as minor micas, pyrite and organic matter (Fig. 4D); while the northupite-cemented mudstone layers (1) and (3) contain irregular K-feldspar and euhedral mica but are intensively cemented and replaced by northupite (Fig. 4E). Notably, there are abundant ash materials floating in salt crystals of the northupite and eitelite layers and no dolomite present in either the evaporite or mudstone layers.

Except for Mg-evaporite laminae and beds, there are many large (>1 mm) nodular or euhedral Mg-evaporite crystals dispersed in mudstone intervals of the lake-central deposits (Fig. 5), making up an important part of the mudstone intervals. Eitelite nodules are the major evaporite occurrence found in the least saline sediments of FC3 (Fig. 5A) and they have been partly altered to Mg-clays (sepiolite; Figs 3A and 5B). Northupite is the most abundant Mg-evaporite mineral in the mudstone intervals of FC2, showing displacive (Fig. 5C) or replacive (Fig. 5D) diagenetic origins. The replacement of shortite by northupite is not a volume-to-volume replacement process (Fig. 5D).

Magnesium-rich minerals of the alkaline lake-transitional zone

The most abundant Mg-mineral in the transitional zone of the Late Palaeozoic saline alkaline lake is dolomite (Fig. 3B), whereas Mg-evaporite minerals are nearly absent, with their existence represented by the presence of many evaporite crystal moulds. Dolomite in the transitional zone appears in two forms; as isolated crystals disseminated within mudstone matrix or as aggregated crystals in bands, nodules or evaporite crystal moulds. Isolated anhedral, subhedral or euhedral dolomite crystals (from 20 μm to *ca* 70 μm in diameter) are variably dispersed within the mudstone matrix (Fig. 6A). These dolomite crystals do not exhibit the thick bright Fe-rich rims (Fig. 6B), that are commonly observed in BSE images of late diagenetic hydrothermal dolomite crystals. When viewed using cathodoluminescence, parts of the isolated dolomite crystals generally have a zoned appearance, with a bright yellow core that is crusted by a thin dark ring, a thick green ring and a dark red outer ring (Fig. 6C and D). In some cases, the isolated dolomite crystals in the Fengcheng Formation also have bright zoned fluorescence (Fig. 6E and F), with a bright yellow core, successively crusted by a dark ring, an orange ring, a green ring, a yellow ring and an outermost dark ring. These dolomite crystals show no signs of transformation from calcium carbonate precursors, and microscopic calcite and aragonite crystals (<70 μm) are almost absent in the Fengcheng Formation.

Dolomite aggregates are also common in the mudstones of the saline alkaline lake transitional zone, which are shaped like evaporite beds, nodules, tepee crusts, roots, desiccation cracks, or dewatering cracks and could be falsely identified

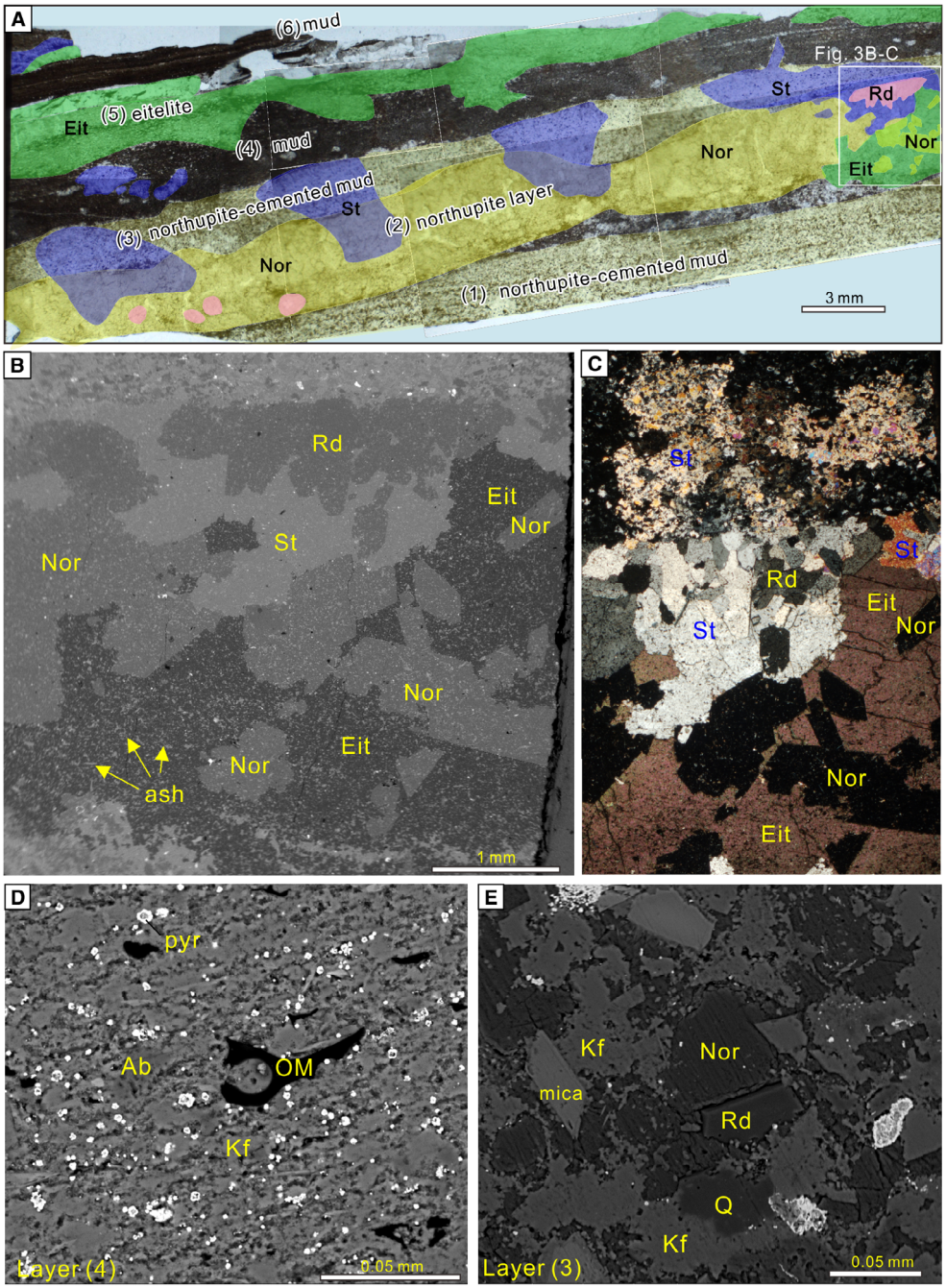

Fig. 4. Fabric details of the laminated Mg-evaporites in the Fengcheng Formation. (A) An interpreted laminated sample alternating with Mg-evaporites and muds, based on backscattered electron (BSE) image scanning (AK1, 5668.89 m, FC1). (B, C) BSE images and photomicrographs (cross-polarized light) used to interpret the paragenesis of minerals in layer (2) – see section on Mg-rich minerals of the saline alkaline lake-central zone – eitelite, northupite, shortite and reedmergnerite. Note the ash materials floating in eitelite and northupite substrates. (D) Details of mud layer (2), showing the main mineral composition as albite and K-feldspar. (E) Details of northupite-cemented mud layer (3) – see section on Mg-rich minerals of the saline alkaline lake-central zone – showing the transformation of K-feldspar to northupite. Ab, albite, Dol, dolomite, Eit, eitelite, Kf, K-feldspar, Nor, northupite, OM, organic matter, Pyr, pyrite, Rd, reedmergnerite, St, shortite.

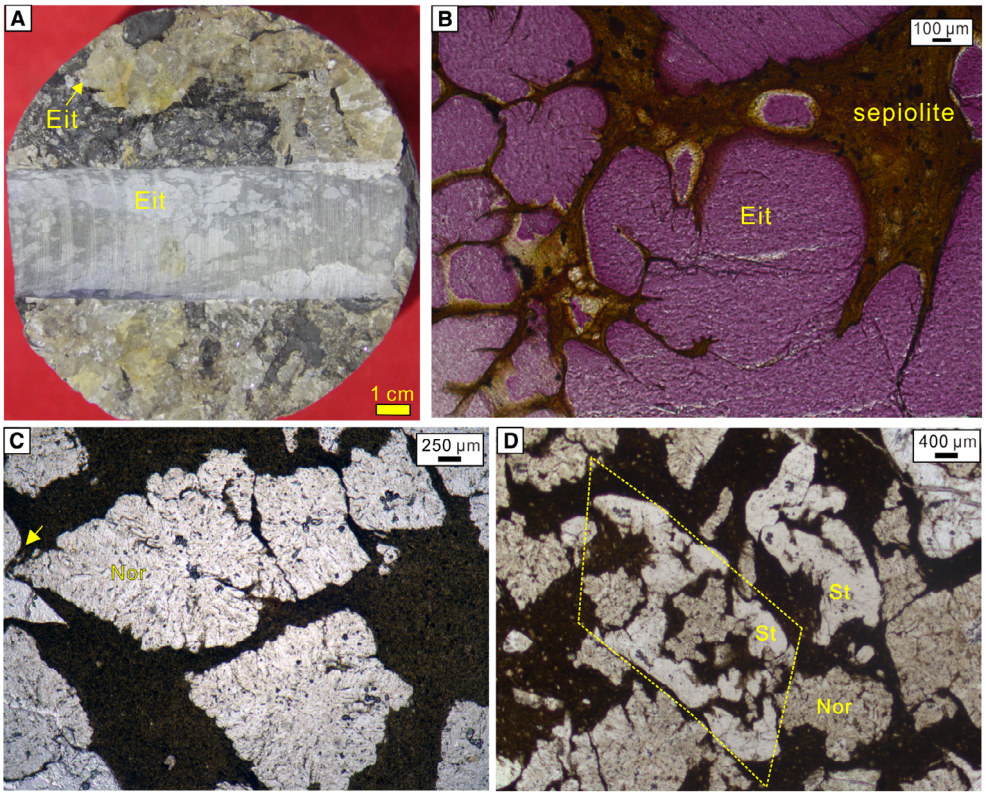

Fig. 5. Magnesium-bearing salts dispersed in the mudstones of the saline alkaline lake centre. (A) and (B) Core photographs and photomicrographs (plane polarized light) showing eitelite nodules inserted in mudstones (F26, 3298.57 m, FC3). Note the transformation of eitelite to sepiolite. (C) Euhedral northupite, an isotropic mineral shaped like a snowflake (FN5, 4071.05 m, FC2). (D) Northupite crystals are replacing a rhombohedral shortite crystal, not in a volume-to-volume manner (FN5, 4068.64 m, FC2). Eit, eitelite; Nor, northupite; St, shortite.

as evaporite crystals by only core observation (Fig. 7A). The existence of discrete evaporite remnants (Fig. 7B) that exhibit uniform extinction under crossed polars, and regular mould shapes (Fig. 7C) demonstrate the previous existence of evaporites. The aggregated dolomite crystals range from 20 μm to over 100 μm in size and have major green cathodoluminescence (Fig. 7D), resembling the luminescence of the thickest ring of the isolated dolomite (Fig. 6D). In some samples where moulds are not totally filled with ankerite-dolomite, it can be observed that dolomite is replacing void-filling calcite.

Magnesium-rich minerals of the alkaline lake-marginal zone

Unlike the mudstones in the lake-transitional zone whose evaporite crystal moulds are mainly filled with aggregated dolomite and/or reedmergnerite (Fig. 7A to D) and whose matrix is disseminated with isolated dolomite (Fig. 6) and reedmergnerite crystals, the mudstones in the lake-marginal zone contain large euhedral calcite-filled evaporite crystal moulds (>1 mm; Fig. 7E) and a dolomite-deficient matrix. These evaporite crystal moulds distort and warp the original mudstone laminae (Fig. 7F), typical of a displacive diagenetic origin. Magnesium was mainly stored in matric clays in the wide flat margin of the Mahu Sag, although the total Mg abundance cannot be very high because the contents of clays in the Fengcheng Formation are relatively low, with most values lower than 10%. Illite, sepiolite and clinochlore are the three major clays detected by XRD in the Fengcheng Formation (Fig. 3B), whose EDS spectra commonly show an apparent peak of Mg and can be uniformly called Mg-clays.

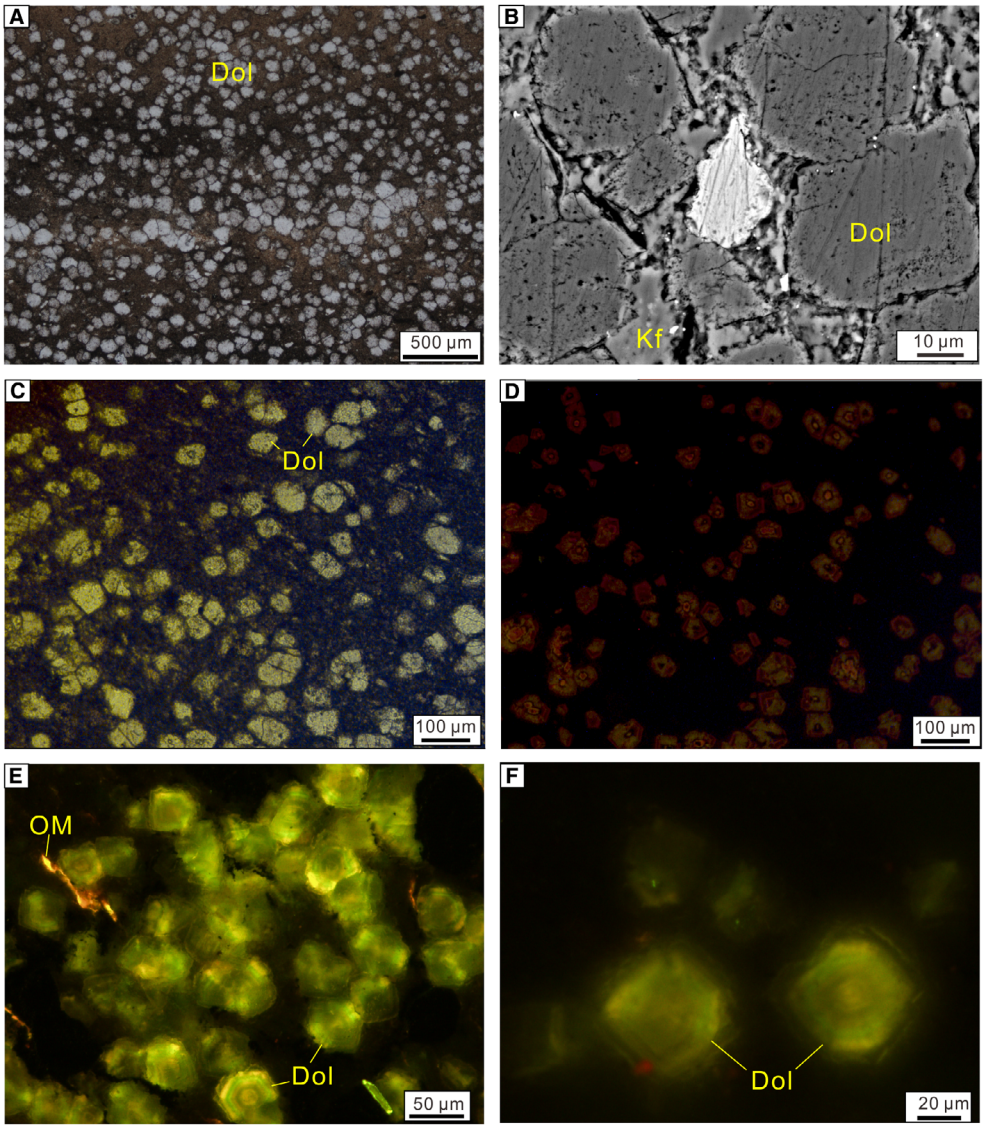

Fig. 6. Fabric details of the disseminated dolomite crystals in the mudstones of the Fengcheng Formation. (A) Dense subhedral dolomite crystals dispersed in mud matrix (FN14, 4085.05 m, FC3). (B) Backscattered electron (BSE) image of disseminated dolomite crystals, showing a near uniform composition without a Fe-rich light ring (MY1, 4591.07 m, FC3); (C) and (D) Same field of view to show cathodoluminescence of disseminated dolomite. Note the zoned luminescence with one or two yellow cores (MY1, 4692.08 m, FC2). (E) Dolomite crystals showing zoned bright fluorescence (MY1, 4596.83 m, FC3). (F) A detailed display of zoned fluorescent dolomites. Dol, dolomite; Kf, K-feldspar; OM, organic matter.

Among the Mg-clays of the Fengcheng Formation, Mg-illite is the most common clay mineral that has been found in every depositional zone, while sepiolite locally occurs in lake-central and transitional zones and clinochlore is locally dominant in lake-marginal zone. Magnesium-illite has varying abundances in the mudstones of different depositional zones and shows a roughly negative correlation with authigenic feldspar and dolomite. Mudstones of the least saline marginal zone are mainly composed of Mg-clays (Fig. 8A) and detrital quartz, K-feldspar and albite, and mudstones of the transitional zone contain abundant authigenic K-feldspar, albite and dolomite crystals dispersed in Mg-illite matrix (Fig. 8B and C). In the lake-central zone

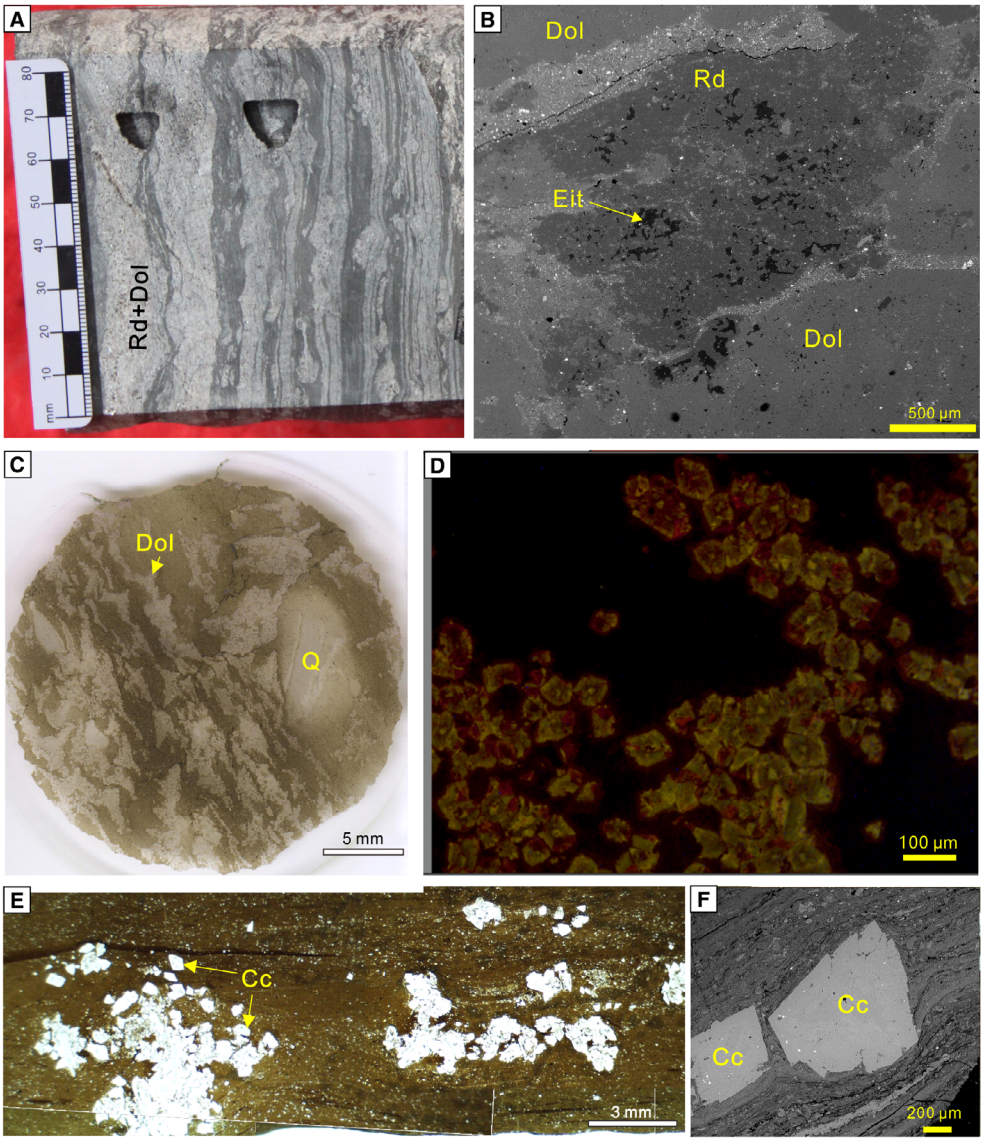

Fig. 7. Evaporite pseudomorph moulds in the Fengcheng Formation, filled with different minerals in different depositional zones. (A) Lake-central core image showing evaporite-like bands and nodules, which are composed of dolomite and reedmergnerite (FC011, 3862.75 m, FC1). (B) Backscattered electron (BSE) images of (A), showing eitelite remnants remained on dolomite and reedmergnerite crystals. (C) Photomicrograph (plane polarized light) of lake-transitional mudstone showing dolomite aggregates dispersed in mud matrix, associated with chert nodules (MY1, 4609.22 m, FC3). (D) Cathodoluminescence image of aggregated dolomite in (C). (E) Photomicrograph (plane polarized light) of a lake-marginal calcitic mudstone (F7, 3156.29 m, FC3). (F) Details of (E), showing calcite pseudomorphs after unknown evaporite minerals. Cc, calcite; Dol, dolomite; Eit, eitelite; Rd, reedmergnerite; Q, quartz.

authigenic K-feldspar and albite dominate the matrix, and Mg-illite is almost absent in mudstone (Figs 4C, 4D and 8D). Sepiolite in the Fengcheng Formation is closely associated with the dissolution of dolomite (Fig. 8E) or eitelite (Fig. 5B) and clinochlore is related to the dissolution of calcite (Fig. 8F).

Carbon and oxygen isotope compositions of carbonates

Different types of carbonate minerals (dolomite, calcite, shortite, northupite, eitelite, trona and wegscheiderite) show similar positive carbon isotopes, ranging from +1 to +7‰, but they

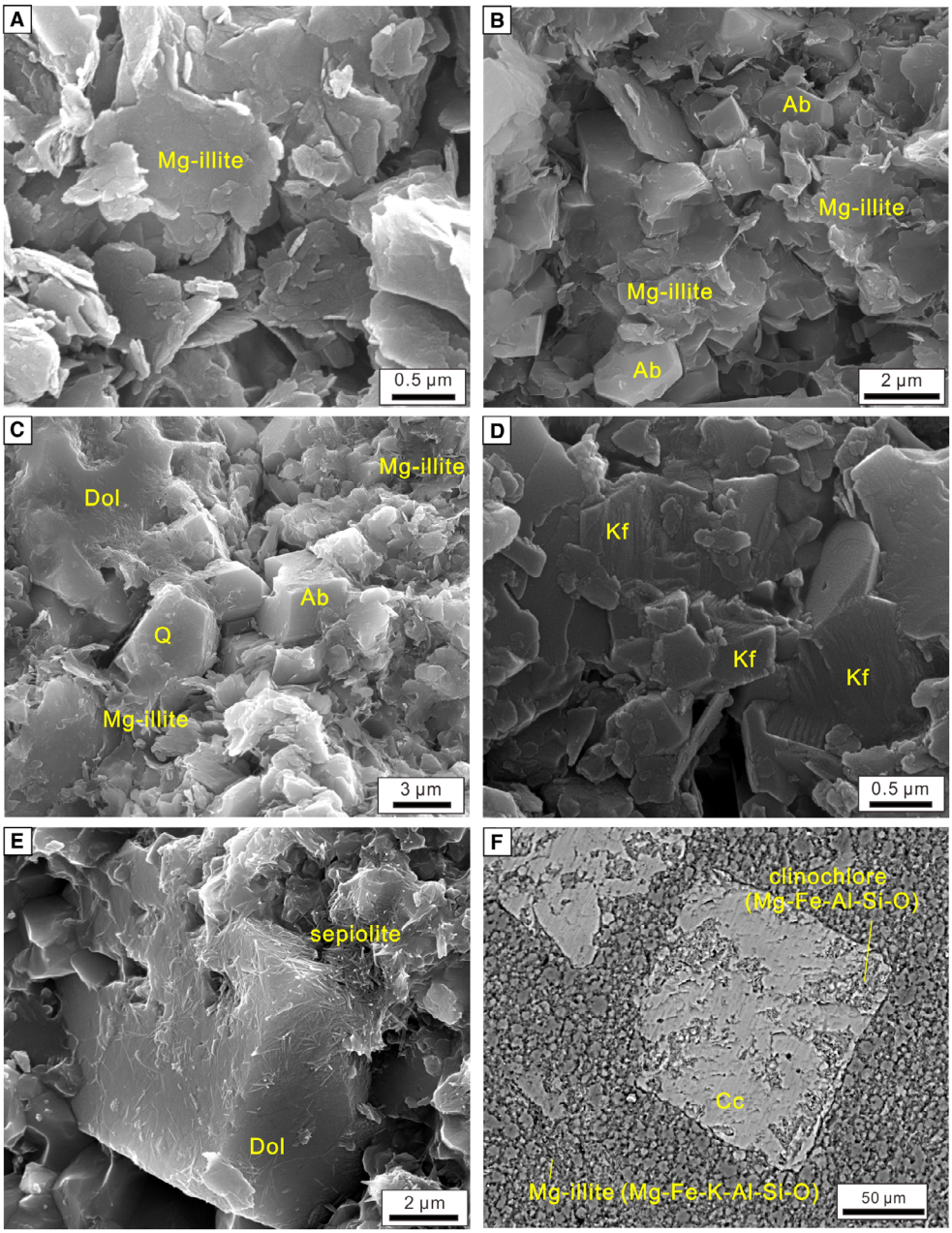

Fig. 8. Scanning electron microscopy (SEM) images showing the fabric details of Mg-clays and their relationships with authigenic feldspar, quartz and dolomite in the mudstones of the Fengcheng Formation. (A) The well-preserved Mg-illite in the lake-marginal mudstone (X40, 4638.12 m, FC2), containing rare authigenic silicates in clay matrix. (B) Authigenic albite crystals developing in Mg-illite matrix in the lake-transitional mudstone (FN14, 4109.47 m, FC3). (C) Authigenic dolomite, albite and quartz developing in Mg-illite matrix of the lake-transitional mudstone (FN14, 4109.47 m, FC2). (D) Matric composition of lake-central mudstone, absent in clays and rich in authigenic K-feldspar (AK1, 5665.99 m, FC1). (E) Sepiolite formation accompanied by the dissolution of dolomite (FN2, 4038.35 m, FC2). (F) The transformation of calcite to clinochlore (F7, 3156.29 m, FC3). Ab, albite; Cc, calcite; Dol, dolomite; Kf, K-feldspar; Q, quartz.

have quite distinctive oxygen isotopes (Fig. 9; Table S1). Sodium-carbonate evaporites (trona + wegscheiderite) and salt-rich (eitelite, northupite and shortite) mudstones are mostly characterized by positive oxygen isotopes ranging from +0.08 to +3.7‰, while two eitelite-bearing

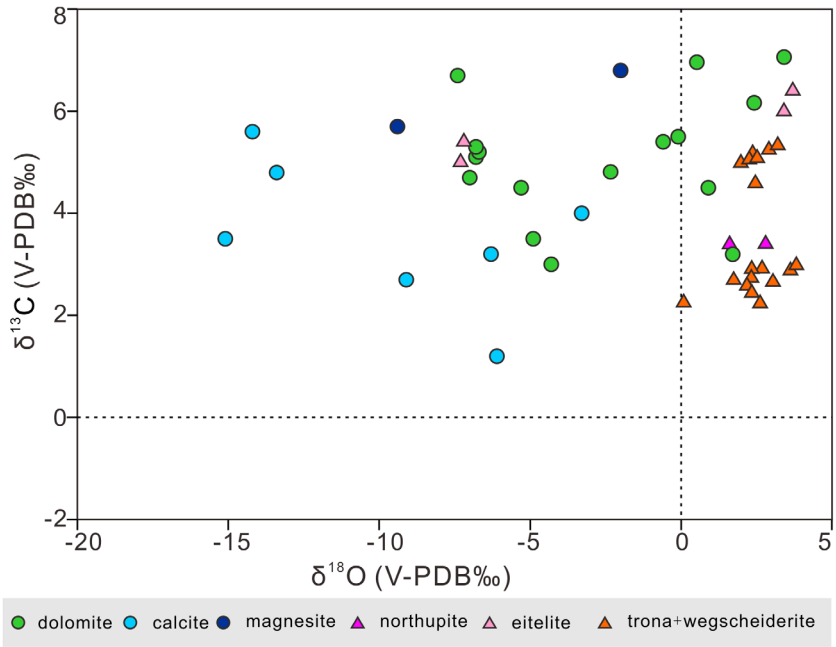

Fig. 9. Carbon and oxygen isotope data of the different carbonate minerals (including Na-carbonate evaporite) found in the Fengcheng Formation.

samples have $\delta^{18}O$ values as low as −7.3‰. Mudstones with abundant mould-filling calcite have the lowest oxygen isotopes (from −15.1 to −3.3‰). Dolomite-bearing and magnesite-bearing mudstones have intermediate $\delta^{18}O$ values between Na-carbonate evaporite and calcite, ranging from −7.4 to +3.4‰.

Magnesium isotopes of magnesium-bearing deposits

Four Mg-rich samples of FC1, including two Mg-evaporite-bearing samples and two dolomite-bearing samples, show an apparent isotopic distinction between Mg-evaporites and their transformed dolomite (Fig. 10A; Table S2). Five Mg-mineral-rich samples of FC2, including two northupite-bearing samples and three dolomite-bearing samples, reveal a narrow range of Mg isotopes from −0.44 to −0.17‰ (Fig. 10A). Nine samples of FC3 display a wide range of $\delta^{26}Mg$ values among Mg-evaporites, dolomite and Mg-clays. Three nodular eitelite samples (Fig. 5A and B) and one sepiolite-bearing sample, collected from the 10 m long core of Well F26, show a wide difference in Mg isotopes (−1.21 to −0.30‰). The transformation degree of eitelite to sepiolite is positively related to $\delta^{26}Mg$ values. Four mudstone samples containing dolomite and Mg-clays as main Mg carriers, show a large distinction in Mg isotopes, which are roughly negatively correlated to dolomite contents. The sample of Well F7 contains Mg-illite as its main Mg-carrier, and shows the heaviest Mg isotope value (+0.7‰).

DISCUSSION

Sources of magnesium in alkaline lake waters

There are variable hypothesized sources for the Mg responsible for the high abundance of authigenic Mg-rich minerals in the alkaline lake deposits of the Mahu Sag. The Late Palaeozoic closed lakes within the Junggar Basin originated from seawater retreat of the Paleodepths Ocean (Carroll *et al.*, 1990), and its water chemistry was later altered by the influxes of magmatic fluids, terrestrial rivers and groundwaters, resulting in uncertainty about the contribution of marine Mg. Magmatic Mg is suggested as an important source for the vast Mg reserve in the Fengcheng Formation, because modern and ancient alkaline lakes are generally related to contemporaneous magmatic activity and its related hydrothermal processes (Lowenstein *et al.*, 2017). In addition, many detrital and pyroclastic silicates become unstable under highly alkaline conditions and will be transformed to Mg-clays, zeolites and feldspars (Hay *et al.*, 1991), releasing more terrestrial Mg than

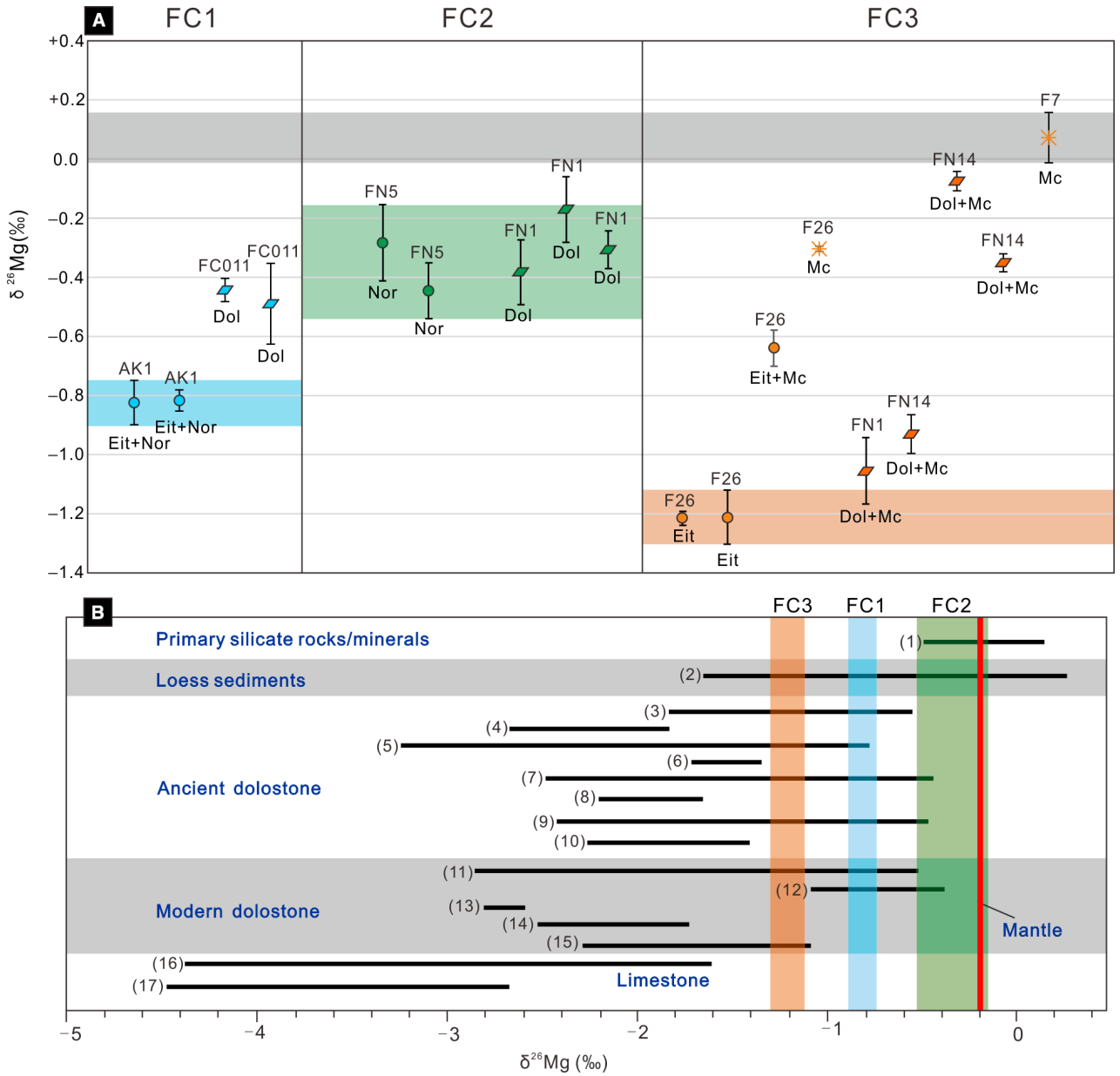

Fig. 10. (A) Magnesium isotopic results of Mg-bearing samples in different members of the Fengcheng Formation in the Mahu Sag. Mg isotopic ranges of Mg-evaporites of different members are highlighted for comparison. Dol, dolomite; Eit, eitelite; Mc, Mg-rich clays; Nor, northupite. (B) Comparison of the Mg isotopes of the Fengcheng Formation deposits with published Mg isotope data. (1) Handler *et al.* (2009), Bourdon *et al.* (2010), Li *et al.* (2010), Teng *et al.* (2010b), Pogge von Strandmann *et al.* (2012). (2) Li *et al.* (2010), Huang *et al.* (2013), Wimpenny *et al.* (2014). (3) Peng *et al.* (2016). (4) Li *et al.* (2016). (5) Lavoie *et al.* (2014). (6) Huang *et al.* (2015). (7) Geske *et al.* (2012). (8) Liu *et al.* (2014). (9) Pokrovsky *et al.* (2011). (10) Geske *et al.* (2012). (11) Blättler *et al.* (2015). (12) Geske *et al.* (2012). (13) Fantle & Higgins (2014). (14) Higgins & Schrag (2010a). (15) Galy *et al.* (2002). (16) Immenhauser *et al.* (2010), Azmy *et al.* (2013), Fantle & Higgins (2014), Kasemann *et al.* (2014). (17) Galy *et al.* (2002). Mantle Mg isotope range is collected from Teng *et al.* (2010a).

that which occurs in other lake types. These transformation processes are controlled by water salinity and pH, which are primarily determined by depositional environments (Hay *et al.*, 1991).

Magnesium isotopes of Mg-rich minerals can provide information about the Mg^{2+} sources of their formation because different Mg-bearing source rocks have distinctive Mg isotopic values

(Fig. 10B). δ^{26}Mg values of the laminated to thinly bedded eitelite and northupite of FC1 (−0.82‰) are lower by 0.3‰ than the nodular dolomite (−0.49 to −0.44‰) that was transformed from nodular eitelite (Fig. 7A and B), indicating that there is possible Mg isotope fractionation between Mg-evaporite and its transformed dolomite. There is also positive Mg isotope fractionation (0.9‰) between eitelite (−1.21‰) and its transformed sepiolite (−0.30‰), as δ^{26}Mg values of eitelite samples of FC3 are positively related to the transformation degrees to sepiolite (Fig. 10A). The Mg isotope fractionation between dolomite and Mg-clays of the Fengcheng Formation is not possible to ascertain because they are common minerals in the lake-transitional mudstones, and it is difficult to separate dolomite isotopic data from that of the Mg-clays via analysis of whole-rock δ^{26}Mg values. In addition, dolomite and Mg-clays in the Fengcheng Formation are genetically related and interconvertible in different diagenetic stages: formation of the isolated dolomite was probably induced by the dissolution of Mg-clays (see *Conditions for dolomite nucleation and growth in alkaline environments* section) and dolomite can be transformed to Mg-clays (sepiolite) in some cases (Fig. 8E). However, since δ^{26}Mg values of the mudstone samples of FC3 are strongly controlled by the relative proportions of Mg-clays to dolomite (Fig. 10A), a negative Mg isotope fractionation is suggested when Mg-clays are transformed into dolomite. Recent studies of Mg isotope fractionation during mineral formation also reveal that Mg-clays are modestly enriched in ^{26}Mg relative to the precipitating solution, whereas Mg-carbonates (Mg-calcite and dolomite) are depleted by 1 to 4‰ (Galy *et al.*, 2002; Tipper *et al.*, 2006; Higgins & Schrag, 2010a, 2010b; Teng *et al.*, 2010b; Tipper *et al.*, 2010; Shirokova *et al.*, 2011). Therefore, considering the isotope fractionations among Mg-evaporites, dolomite, and Mg-clays and the primary and very early diagenetic origins of Mg-evaporites, the δ^{26}Mg values of Mg-evaporites were selected to represent the information of Mg sources of primary lakes. Comparatively, δ^{26}Mg values of the Mg-evaporites of FC2 (−0.44 to −0.28‰) are higher than those of FC1 (−0.82‰) and FC3 (−1.21‰) (Fig. 10A), indicating that the precipitation solution (lake water) of FC2 was enriched in the heavy ^{26}Mg, successively followed by the FC1 and FC3 solutions.

Overall, Mg-bearing minerals of the Fengcheng Formation, of primary or early diagenetic origins, are more enriched in ^{26}Mg (−1.21 to −0.28‰) than previously reported ancient marine limestones (−4.4 to −1.4‰) (Galy *et al.*, 2002; Immenhauser *et al.*, 2010; Azmy *et al.*, 2013; Fantle & Higgins, 2014; Kasemann *et al.*, 2014; Fig. 10B). They also have, on average, (−0.55‰) higher δ^{26}Mg values than most reported from ancient marine dolostones (−3.2 to −0.4‰; Pokrovsky *et al.*, 2011; Geske *et al.*, 2012; Lavoie *et al.*, 2014; Liu *et al.*, 2014; Huang *et al.*, 2015; Li *et al.*, 2016; Peng *et al.*, 2016) and modern marine dolomite (−2.8 to −0.4‰; Galy *et al.*, 2002; Higgins & Schrag, 2010a; Geske *et al.*, 2012; Fantle & Higgins, 2014; Blättler *et al.*, 2015) (Fig. 10B). The range of δ^{26}Mg values of the Fengcheng Formation evaporites (−1.21 to −0.28‰) overlaps with reported values for palaeosol and loess (−1.2 to +0.25‰, Li *et al.*, 2010; Huang *et al.*, 2013; Wimpenny *et al.*, 2014), and is lower than the reported values for silicate rocks (−0.5 to +0.2‰, Handler *et al.*, 2009; Bourdon *et al.*, 2010; Li *et al.*, 2010; Teng *et al.*, 2010b; Pogge von Strandmann *et al.*, 2012; Fig. 10B) and mantle (−0.2‰, Teng *et al.*, 2010a). These comparisons suggest an important proportion of more radiogenic Mg sources from terrestrial silicate rocks and/or magmatic fluids for the ancient alkaline lacustrine system of the Fengcheng Formation. Because lake water alkalinity and salinity were highest during FC2 deposition and magmatic activity was most intensive during FC1 deposition, the higher Mg isotopes of FC2 Mg-evaporites (−0.44 to −0.28‰) than those of FC1 evaporites (−0.82‰) suggests that water alkalinity and salinity mainly controlled the ^{26}Mg enrichment in these alkaline lakes. Such control has been suggested based on the dissolution capacity of terrestrial and pyroclastic silicates. Comparatively, the FC3 lake water was less saline and alkaline, and underwent the weakest volcanic activity, so it received poor Mg sources.

Sink and stabilization of magnesium in alkaline lakes

Direct precipitation of magnesium-rich minerals from water columns

The presence of bedding or lamination for authigenic minerals is generally indictive of a primary origin, representing direct precipitation from lake waters (Ortí *et al.*, 2016). In the Fengcheng Formation, only the two main Mg-evaporites, eitelite and northupite, show distinct lamination or bedding structures and are

interbedded with salt-bearing mudstone intervals (Fig. 4), suggesting a high probability that they were two effective Mg-carriers to sink Mg^{2+} ions from lake waters into sediments. Both anhydrous Mg-Na-carbonates can directly precipitate from solution under Earth's surface conditions, in contrast to dolomite and magnesite. Primary northupite has been reported in modern Lake Mahega, Uganda (Kilham & Melack, 1972) and in Holocene deposits of Lake Searles in California, USA (Smith & Stuiver, 1979). Northupite is the default Mg-bearing salt and precipitates in large amounts beginning at *ca* 0.9 $a H_2O$ salinity at all temperatures and CO_2 concentrations (Olson & Lowenstein, 2021). Eitelite laminae and beds have been reported in six boreholes from the Eocene Green River Formation, Colorado, USA (Dyni, 1996) and in Holocene sediments from a crater lake at Malha, north-west Sudan (Mees *et al.*, 1991), both of which have been reported as authigenic minerals. In the Fengcheng Formation, the microscopic eitelite crystals, forming a lamina, are not replacive diagenetic products but primary precipitates (Fig. 4A). The floating tiny tuff materials that remained in eitelite laminae (Fig. 4B) indicate a continuous supply of airborne tuffs into lakes when eitelite crystallized from lake waters. Rapid precipitation and growth of eitelite crystals diluted the settling down of ash materials and, as a result, the original laminae mainly consisted of eitelite and tuffs.

The northupite laminae in the Fengcheng Formation, however, were mainly formed by intensively replacing eitelite laminae since small particles of residual eitelite substrate, displaying the same extinction under crossed polars have been found in the northupite laminae (Fig. 4B and C). Northupite is the only important Cl-bearing mineral found in the Fengcheng Formation, while bedded halite, another common Cl-bearing mineral in nature, has not been cored so far, suggesting that the alkaline lake within the Mahu Sag was not saline enough to directly precipitate northupite and halite from primary waters. Northupite in the Green River Formation of Wyoming formed in response to a decrease either in $a CO_2$ or $a H_2O$, or both (Bradley & Eugster, 1969; Olson & Lowenstein, 2021). The replacement of eitelite laminae by northupite in the Fengcheng Formation, could be the result of post-depositional increases of porewater salinity during compaction and a decrease in $a H_2O$, which resembled the formation mechanism of microcrystalline halite in mud intervals of the Lake Searles deposits (Smith & Stuiver, 1979). The post-depositional concentration of Cl-rich-solutions, in buried sediments was caused by the salt-filtering effect of compacting clays, which acted as a membrane that allowed H_2O to escape during compaction more rapidly than the salts dissolved.

Formation of magnesium-rich minerals within sediments

Except for the bedded or laminated eitelite, other Mg-rich minerals in the Fengcheng Formation, including northupite, dolomite and Mg-clays, are present mostly as isolated nodules, disseminated crystals, cements or matrix components in mudstone intervals, which can be interpreted as replacive or displacive diagenetic minerals (Smith & Stuiver, 1979). The decreasing trends of oxygen isotopes from lake-central evaporites (+0.08 to +3.7‰) to lake-transitional dolomite-bearing mudstones (−7.4 to +3.4‰) and to lake-marginal calcite-bearing mudstones (−15.1 to −3.3‰; Fig. 9) suggest that water salinity of the primary lake determined the types of carbonate minerals forming in mudstones, indicative of early diagenetic products forming near the water–sediment interface or in the shallow subsurface. The absence of minerals directly precipitating from water columns can result from thermodynamic limitations due to undersaturation of fluids and/or from kinetic barriers if ambient fluids have reached high supersaturation degrees. The former situation is fitting for the northupite in the mudstone intervals of the Fengcheng Formation, which can crystallize under Earth's surface temperature and has no kinetic inhibitor (Kilham & Melack, 1972; Olson & Lowenstein, 2021). The isolated euhedral northupite crystals present in the matrix of the lake-central mudstones, replacing shortite (Fig. 5C) or not (Fig. 5D), are interpreted as results of total replacement of Na-Ca-carbonate and authigenic growth in matrix. Except for Mg-evaporites, other Mg-rich minerals, such as dolomite, palygorskite, sepiolite and Mg-smectite, are difficult to directly precipitate from lake waters due to either kinetic or thermodynamic inhibitors (Kaczmarek *et al.*, 2017; Milesi *et al.*, 2019). They fail to be synthesized in the laboratory at Earth surface temperatures and pressures (Ryan *et al.*, 2019). As a result, the vast majority of Mg^{2+} ions in the alkaline lake of the Fengcheng Formation were stabilized by minerals within sediments in the shallow subsurface, via replacive or displacive diagenesis.

In the transitional zone of the saline alkaline lake, dolomite occurs as isolated dispersed or aggregated crystals and is the dominant Mg-rich mineral (Figs 6 and 7). Isolated dispersed dolomite is a common mineral component in saline lake siliciclastic sediments (Last, 1990) and it can be present in various lithofacies, such as deep-water laminates and marginal-playa mudstones. Genesis of such dolomite is generally controversial and suggested hypotheses include primary dolomite (Smith & Stuiver, 1979; Wen *et al.*, 2020), penecontemporaneous dolomite (Wolfbauer & Surdam, 1974), organogenic dolomite (Slaughter & Hill, 1991; Mazzullo, 2000), detrital dolomite (Eugster & Surdam, 1973) and hydrothermal primary dolomite (Wen *et al.*, 2013; Yang *et al.*, 2020). In the Fengcheng Formation, the isolated dispersed dolomite crystals show zoned cathodoluminescence (Fig. 6C and D) and zoned fluorescence (Fig. 6E and F), indicating that these dolomite crystals have undergone several stages of overgrowth. The cores of isolated dolomite crystals have dulled red to yellow luminescence and bright yellow fluorescence, which can be interpreted as a primary microbially-mediated mineral phase forming in a weakly oxidizing to weakly reducing diagenetic environment. Degradation/decomposition of organic matter in a near-surface system by aerobic heterotrophic, sulphate reducing and/or methanogenic bacteria can produce CO_2 and enhance carbonate alkalinity, which can induce dolomite precipitation from interstitial waters (Vasconcelos & McKenzie, 1997; Roberts *et al.*, 2004; Sánchez-Román *et al.*, 2008, 2009b, 2011a; Meister *et al.*, 2011). This primary dolomite hypothesis is supported by the absence of microscopic calcite or aragonite precursors in both dolomite-rich and dolomite-absent mudstones of the Fengcheng Formation. The fluorescent dolomite cores resemble the primary microbial dolomite within stromatolites in Miocene lacustrine deposits from the Duero Basin, Spain (Sanz-Montero *et al.*, 2008), the primary dolomite associated with gypsum in Miocene evaporitic lake deposits of the Madrid Basin, central Spain (Sanz-Montero *et al.*, 2006), and the modern and late Holocene dolomite in Manito Lake, Saskatchewan, Canada (Chahi *et al.*, 1999). Except for the fluorescent cores, the isolated dolomite crystals of the Fengcheng Formation also have zoned fluorescent rims, implying that there was also organic matter in dolomite rims and their continued growth within the matrix was also aided by microbial activity. The thick olive-green luminescence of the dolomite rims (Fig. 6D) suggests that their continued growth environments were more reducing and deeper than their nucleation environments. The outermost thin rings of the dolomite crystals have dark red luminescence (Fig. 6D) and weak fluorescence (Fig. 6F), indicating that the last growth stages of dolomite were in a reducing, organic-lean diagenetic environment, corresponding to a late diagenetic stage. Therefore, the isolated dolomite crystals finished nucleation and major growth in an early diagenetic stage aided by anaerobic microbial degradation of organic matter, which can be interpreted as organogenic dolomite (Slaughter & Hill, 1991; Mazzullo, 2000).

The co-enrichments of isolated dispersed dolomite and aggregated dolomite in the mudstones of the lake-transitional zone suggest that they were genetically related. The olive-green luminescence of the aggregated dolomite (Fig. 7D) resembles the luminescence of the thick ring of isolated dispersed dolomite in mudstone matrix (Fig. 6D), also implying that they formed in similar diagenetic environments and possibly coevally. The dolomite aggregates were mainly filled in tepee horizons, shrinkage cracks, and evaporite crystal moulds (Fig. 7A to D; Guo *et al.*, 2021), which were formed in pedogenetic or shallow water environments that frequently suffered subaerial exposures. During dry seasons, evaporite crusts, nodules and shrinkage cracks were developed, which would be dissolved during following flooding seasons. Calcite was generally the first void-filling mineral after evaporite dissolution, which is the case in lake-marginal mudstone of the Fengcheng Formation (Fig. 7E). Similar large calcite pseudomorphs after evaporites in mud/tuff beds have been identified in other Permian strata in the southern Junggar Basin (Hackley *et al.*, 2016), which was deposited in an alkaline lake less saline than the one in the Mahu Sag. In the following diagenetic stages, the void-filling calcite could be easily dolomitized if porewaters were mixed with higher-salinity water. The pervasive dolomitization of void-filling calcite in the transitional zone might result from water mixing of high-salinity lake water and low-salinity groundwater during lake transgression after a lake level drop, or from the dissolution of other Mg-rich minerals (Zhu *et al.*, 2017), resembling the dolomite origins within the Cretaceous pre-salt carbonates on the south Atlantic coastal margins (Tosca & Wright, 2015).

In the lake-marginal deposits of the saline alkaline lake, Mg-clays become the dominant Mg-rich minerals, not because their contents are very high but because other Mg-rich minerals, like dolomite and Mg-evaporites, are rare in this depositional zone (Fig. 7E). Magnesium-clays in alkaline playa-lake environments can be produced by reaction of volcanic materials with alkaline waters (Surdam & Parker, 1972), by transformation from detrital clay minerals in contact with alkaline waters (Hay & Guldman, 1987; Bristow *et al.*, 2012), or by neoformation via the aid of microbes in microbial mats (Perri *et al.*, 2018). Whether Mg-rich clays are Al^{3+}-rich or Al^{3+}-poor in alkaline lake deposits depends on water chemistry (pH, salinity, Mg/Si ratios) and the lithology of host sediments (Al^{3+}-rich or not; Pozo & Calvo, 2018). Transformation of detrital clays was suggested as the dominant pathway for the formation of Mg^{2+}-rich clays in the Fengcheng Formation because the presence of foreign surfaces of detrital clay minerals contribute to lowering the interfacial energy required for nucleation of Mg-silicates (Pozo & Calvo, 2018). Petrological evidence reveals that the uncommon Mg-clays in the Fengcheng Formation, sepiolite and clinochlore, were apparently transformed from eitelite (Fig. 5A and B), dolomite (Fig. 8E) and calcite (Fig. 8F), whereas the reasons for and timing of these transformations remain poorly studied. The more common Mg-illite of the Fengcheng Formation has several possible origins. Both detrital clays and volcanic materials could become unstable in highly alkaline saline environments and be transformed to other silicates, like Mg-smectite, Mg-illite, zeolite and K-feldspar (Surdam & Parker, 1972; Hay & Guldman, 1987; Hay *et al.*, 1991). Transformation of detrital clays or tuff materials to Mg-smectite had probably finished near the water–sediment interface or in the very shallow subsurface. This is because porewater chemistry analysis of modern alkaline lake sediments (Lake Turkana, Kenya) shows a dramatic increase of Mg concentration at *ca.* 5.5 m below the water–sediment interface due to the dissolution of generated Mg-silicates (Cerling, 1996). Also Mg-smectite would be readily transformed to Mg-illite when strata temperature increased during deep burial. Such a process in the Fengcheng Formation might not need high temperature and pressure, or to occur at burial depths, because in alkaline saline lakes with an unusually high K/Na ratio diagenetic illization occurred parallel to the process of analcime formation (Singer & Stoffers, 1980).

Conditions for dolomite nucleation and growth in alkaline environments

Weak competitiveness for magnesium by dolomite

Laterally, dolomite of the Fengcheng Formation, regardless of mineralogical occurrences, is rare in the most condensed depositional environment (lake centre), and stratigraphically, dolomite shows the highest enrichment in the least saline stage (FC3), demonstrating that the concentrations of bulk Mg^{2+} ions in primary alkaline lakes did not determine the dolomite abundance in deposits. This phenomenon is in accordance with the scarcity of dolomite in modern marine deposits although seawaters are supersaturated with respect to ordered dolomite (Raudsepp *et al.*, 2022). The difficulty for low-T dolomite formation mainly resides in the strong hydration of Mg^{2+} ions (Zhang *et al.*, 2012; Shen *et al.*, 2014; Kaczmarek *et al.*, 2017; Wen *et al.*, 2020; Fang & Xu, 2022), which, however, seemed not to be a big constraint for the formation of other Mg-rich minerals in alkaline environments. The direct precipitation of anhydrous Na-Mg-carbonate (eitelite) from lake waters, as well as the displacive diagenetic formation of northupite near the water–sediment interface, suggests that there were enough free Mg^{2+} ions in the saline alkaline lakes of the Fengcheng Formation available for Mg-Na-carbonate formation. This availability of free Mg^{2+} ions might result from the high ionic strength in highly saline alkaline waters (Vandeginste *et al.*, 2019). There is an apparent positive relationship between pH and Mg contents in synthetic amorphous Ca-Mg-carbonate and when pH reaches 10.3, the Mg content can reach 65% (Blue & Dove, 2015). The great abundance of free Mg^{2+} ions in alkaline water could also be related to the elevated concentration of dissolved silica, which possesses low-dipole moment and dielectric constant similar to hydrogen sulphide, dioxane, polysaccharide and exopolymeric substances (EPS) and can lower the dehydration energy barrier of a surface Mg^{2+}–H_2O complex (Hobbs & Xu, 2020; Fang & Xu, 2022; Fang *et al.*, 2023). This hypothesis can be ascertained by the close association of dolomite and cherts in the Fengcheng Formation, although further work needs to be done. Therefore, the paucity of dolomite in the Fengcheng Formation of lake-central zone cannot be mainly ascribed to the strong hydration of Mg^{2+} ions and the low availability of free Mg^{2+} ions.

In the Fengcheng Formation, after the primary eitelite precipitates had sunk parts of Mg^{2+} ions from lake waters, the remaining Mg^{2+} ions were left in porewaters or adsorbed by organic matter and clays within buried sediments, which were readily incorporated into Mg-rich minerals, such as Mg-Na-carbonates, Ca-Mg-carbonates or Mg-clays. The similar Mg isotopes of early diagenetic northupite (−0.28 to −0.44‰) and dolomite (−0.17 to −0.55‰) of FC2 indicate similar Mg sources and the existence of mutual competition for Mg^{2+} ions in porewaters. In lake-central sediments, isolated dispersed dolomite crystals can be present in shortite-bearing and reedmergnerite-bearing mudstones, but they seldom occur in northupite-bearing mudstones (Figs 4C and 5C to F). It is, thus, suggested that isolated dolomite can form in saline intervals, but cannot generate during diagenetic Mg-evaporite formation. The same situation has been observed in Holocene sediments from Lake Searles, where dolomite is absent in northupite-bearing horizons (Smith & Stuiver, 1979). In the lake centre of the Fengcheng Formation, detrital clays and authigenic Mg-clays are almost absent in mudstones while authigenic K-feldspar crystals are the dominant matric components (Figs 4E, 5C, 5D and 9D), which is consistent with the lateral distribution of authigenic silicates in alkaline lakes (Surdam & Parker, 1972; Hay & Guldman, 1987). The interaction of tuff beds or detrital clays with basinward increasingly saline and alkaline waters will produce a zonation of authigenic silicates, which are, from lake margin to centre, Mg-smectite, clinoptilolite, analcime and K-feldspar + searlesite (Surdam & Parker, 1972; Hay & Guldman, 1987). Magnesium-clays and zeolites will further be altered to K-feldspar and searlesite when interacting with lake-central highly saline, alkaline pore fluids containing abundant K^+ and Na^+ ions (Surdam & Parker, 1972; Hay & Guldman, 1987; Hay *et al.*, 1991). Therefore, in the subsurface of the lake centre, Mg is probably incorporated more easily, faster or earlier into Na-Mg-carbonate lattice together with Cl^- ions than into Ca-Mg-carbonate and Mg-clays.

In the northupite-free mudstones of the lake-transitional to marginal zones, the waxing and waning of isolated dispersed dolomite and Mg-clays in mudstones strongly suggest that they were genetically linked. Due to the lower porewater salinity of lake-transitional to marginal sediments as suggested by oxygen isotopes (Fig. 9), the inherited Mg^{2+} ions from lake waters were also fewer in abundance than the porewaters of lake-central sediments. Under such circumstances, some studies suggested that the transformation of detrital clays to Mg-clays in highly alkaline conditions can uptake porewater Mg^{2+} ions faster than dolomite; as a result, dolomite abundance can be enhanced only when the influx of terrestrial clays is limited (Bristow *et al.*, 2012). While other studies suggested that there was no direct competition for Mg^{2+} ions between dolomite and Mg-clays in alkaline lake sediments, because these two types of Mg-rich minerals were formed under different hydrochemical conditions (Ryan *et al.*, 2019), Chase *et al.* (2021) hypothesized a theoretical Mg-mineral precipitation line defined by amorphous silica saturation and the critical supersaturation for Mg-silicate nucleation, above which Mg-clays will precipitate and below which Mg-carbonates (high-Mg calcite, hydromagnesite, or other metastable hydrated Mg carbonate phases) will precipitate. In the Fengcheng Formation, the total contents of clays are generally low (<10%) and show a basinward decrease, in contrast to the basinward increase of authigenic albite and K-feldspar contents (Fig. 8A to D). Because the materials for the formation of authigenic albite and feldspar in alkaline lake diagenetic systems can be sourced from the transformation of detrital clays (Hay *et al.*, 1991) and dissolution of Mg-clays (Tosca & Wright, 2015; Wright & Barnett, 2015), the present content of Mg-illite was not only controlled by the abundance of detrital clays, but also related to how much it has been transformed. In the lake-transitional zone where dolomite, authigenic K-feldspar and albite are abundant, Mg-illite matrix was largely reduced (Fig. 8B and C), suggesting that the authigenesis of K-feldspar, albite and dolomite was related to the transformation of Mg-smectite and Mg-illite. Thus, it is agreed that in overall alkaline conditions (pH > 9) with a high influx of Al^{3+}-rich silicates, Mg-clays will precipitate over dolomite in the water column and near the sediment–water interface and consume the Mg^{2+} ions in interstitial fluids.

Therefore, although highly alkaline environments are supposedly very favourable for low-temperature dolomite formation, it is still not easy for dolomite formation and enrichment to happen. This is because dolomite is at a competitive disadvantage for Mg compared to Mg-evaporites when water salinity is simultaneously high and to Mg-clays when salinity is low

(Fig. 11). This weak competitiveness might arise from the intrinsic barrier that stems from the lattice limitation on the spatial configuration of CO_3 groups in both magnesite and dolomite crystals (Xu *et al.*, 2013; Zhou *et al.*, 2021) or the difference in cation properties (Pimentel & Pina, 2016), which cause the nucleation and growth rates of low-temperature dolomite much slower than those of Mg-evaporites and Mg-clays. Age determination of dolomite by C^{14} methods in the surficial sediments of Deep Spring Lake, California, indicated that the average growth rate of individual dolomite crystals is very slow, on the order of hundreds of angstroms per thousand years (Peterson *et al.*, 1963). It has also been proved that magnesite formation is a reaction-controlled process even in highly supersaturated solutions and its estimated rates in alkaline playas are in the range of 10^{-17} to 10^{-16} mol/cm^2/s, which is much slower than those of hydrous carbonates, calcite and aragonite (Power *et al.*, 2019). Therefore, even under supersaturated conditions, the nucleation and growth of dolomite would proceed very slowly, giving rise to the predominant consumption of Mg^{2+} ions by northupite and Mg-clays.

The limitation of dolomite formation within lake water columns or near the Earth's surface in highly alkaline lakes might also be attributed to phosphate inhibition of calcium carbonate precipitation and the rarity of finely particulate (micritic) calcite or aragonite precipitates (Pietzsch *et al.*, 2022). High alkalinity can enhance the accumulation rate of phosphate in lake waters, and phosphate is the most effective inhibitor to suppress the nucleation of new $CaCO_3$ and promote growth of calcite crystals on pre-existing substrates in the Cretaceous alkaline lakes along the South Atlantic margin (Pietzsch *et al.*, 2022). The enhanced phosphate inhibition of calcium carbonate precipitation by high alkalinity can explain the rarity of microscopic calcite and aragonite (<70 μm) in the Fengcheng Formation, not only in the dolomite-rich

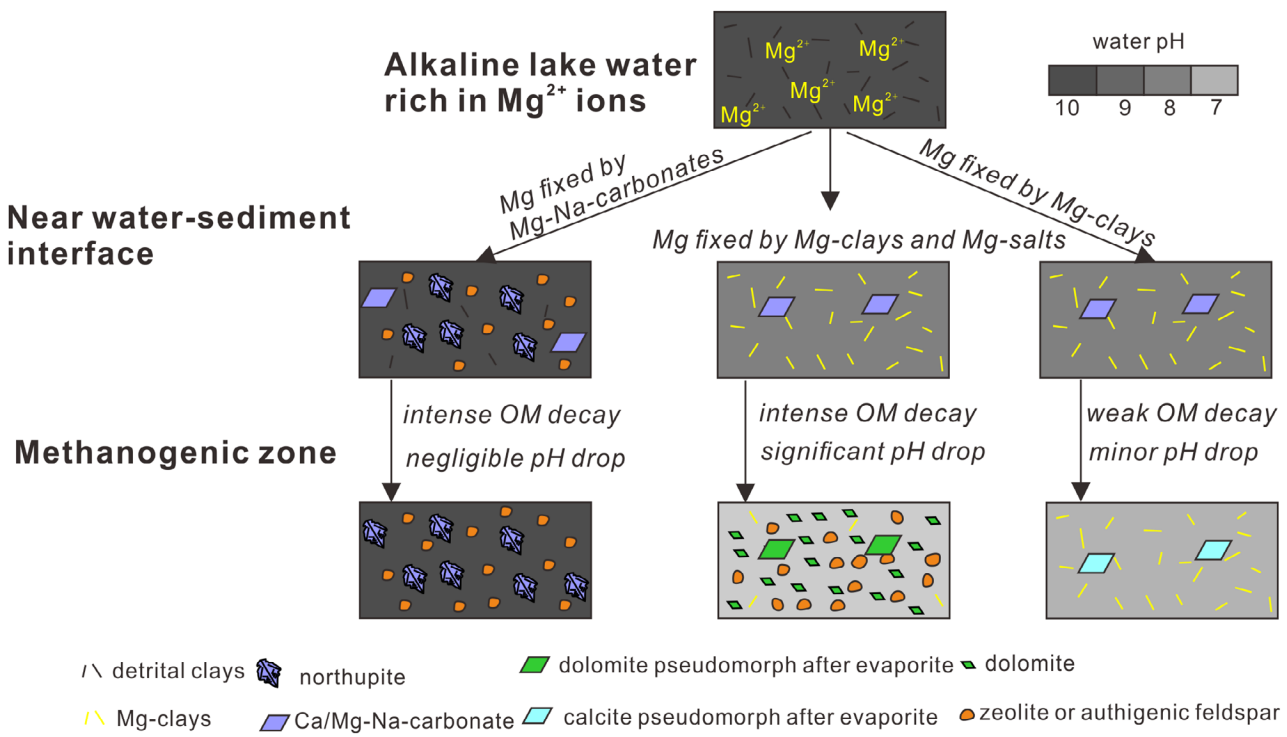

Fig. 11. The fates of Mg^{2+} ions in different depositional zones of a saline alkaline lake, illustrating the influence of the formation and diagenesis of eitelite, northupite and Mg-clays and the microbial degradation of organic matter on dolomite nucleation and growth. The large crystal size (20 to 70 μm) and enrichment of dolomite in the transitional zone are attributed to the methanogenic degradation of organic matter and the resultant effective decrease of porewater pH, which cannot be realized in lake-central deposits due to the existence of abundant acid-buffering Na-carbonate evaporites and also in lake-marginal deposits due to the low abundance of organic matter and weak methanogenesis. OM, organic matter.

mudstones, but also in the dolomite-deficient mudstones. Calcite of the Fengcheng Formation mainly occurs as a void-filling mineral, forming after the dissolution of Na-carbonate evaporites. As a result, rare precursor phases, including amorphous phases, crystalline nano-particles, metastable Ca-Mg-carbonates with varying Ca/Mg ratios (high magnesium calcite, very high magnesium calcite, disordered dolomite) are available for the formation of ordered dolomite (Meister & Frisia, 2019; Raudsepp *et al.*, 2022). The failed nucleation of calcium carbonates will facilitate the incorporation of Ca into hydrous Ca-Na-carbonates, such as gaylussite and pirssonite, which further prevent Ca from entering Ca-carbonates and Ca-Mg-carbonates. An alternative explanation for the deficiency of microscopic calcite and aragonite (<100 μm) in the Fengcheng Formation could be that calcite and aragonite had precipitated from the water column but were later completely dissolved or replaced by dolomite during diagenesis. Analysis of porewater chemistry of the sediments in the alkaline Lake Turkana, Kenya, found that newly-precipitated calcite would be partly dissolved due to the increased high $p(CO_2)$ and decreased porewater pH during methanogenesis (Cerling, 1996). In some lakes dissolution induced by methanogenesis and CO_2 production probably leads to a complete removal of primary carbonate precipitates (Talbot & Kelts, 1990). Since microscopic calcite is nearly absent in both organic-rich and organic-lean mudstones, this precipitation and dissolution proposition was unlikely to be the case for the Fengcheng Formation.

Catalyst for dolomite nucleation and growth

Despite the weak competitiveness of dolomite with respect to Mg-evaporites and Mg-clays in highly alkaline lakes, dolomite is surprisingly very enriched in the transitional zone of the saline alkaline lake (Figs 6 and 7), suggesting the existence of extra catalyst(s) for dolomite nucleation and overgrowth there. Such supposed catalyst(s) should enable dolomite to compete for Mg^{2+} ions from porewaters or could cause the dissolution of generated Mg-evaporites and Mg-clays to re-release the stabilized Mg for subsequent dolomite formation. Given the coeval resulting instability of Mg-evaporites and Mg-clays, the main function of the catalyst(s) was most likely to induce the decrease of porewater pH, because both Mg-clays and Na-Mg-carbonates are unstable when pH drops to below 8 (Tosca & Wright, 2015; Zhu *et al.*, 2017). In the shallow subsurface, the drop of porewater pH can be caused by a variety of biogeochemical processes, such as respiration reactions, most re-oxidation reactions, mineralization processes of organic matter by sulphate reduction, methanogenesis and anaerobic methane oxidation (Cerling, 1996; Soetaert *et al.*, 2007; Meister, 2013; Tosca & Wright, 2015; Wright & Barnett, 2015), among which the mineralization processes of organic matter in decreasing pH are conditional, depending on the initial solution pH (Soetaert *et al.*, 2007). At high pH values (>7), the CO_2 produced by sulphate reduction, methanogenesis or anaerobic methane oxidation will be hydrolyzed to produce protons and lower the pH; whereas at low pH values, the small negative charge produced by inorganic carbon is surpassed by the positive charge (ammonium, NH_4^+) (Soetaert *et al.*, 2007). In some modern alkaline lakes, porewater pH can be even dropped to *ca* 7 below the water–sediment interface due to organic matter decomposition (Fussmann *et al.*, 2020). Bacterial degradation will be enhanced by high contents of organic matter in sediments (Mazzullo, 2000), which is also supported by the close association of dolomite abundance with organic matter content in the Fengcheng Formation (Guo *et al.*, 2021). In the mudstone intervals containing little organic matter (alginite), microscopic dolomite is absent and Mg-illite matrix is abundant; whereas in the mudstone intervals with abundant lamalginite, microscopic dolomite crystals, plus authigenic K-feldspar and albite (Fig. 8B and C), are also abundant (Guo *et al.*, 2021), suggesting that the organic matter diagenesis promoted dolomite formation. Because porewater pH could be effectively buffered by the vast inherited dissolved inorganic carbon of alkaline lakes (Soetaert *et al.*, 2007; Meister, 2013), the saturation states with respect to carbonate minerals are slightly increased and the newly nucleated dolomite was not susceptible to dissolution. It is, thus, suggested that organic-poor sediments are not favourable for primary dolomite formation in alkaline lacustrine sediments as has been previously suggested (Baker & Burns, 1985; Sánchez-Román *et al.*, 2009a, 2011b; Petrash *et al.*, 2016).

Since dolomite in the Fengcheng Formation shows uniformly positive carbon isotopes (+3.0 to +6.2‰) and negative to slightly positive oxygen isotopes (Fig. 9), bacterial methanogenesis, instead of bacterial sulphate reduction, is suggested as the major anaerobic organic

degradation process driving dolomite formation (Zhu *et al.*, 2017). In alkaline lakes, the combination of low dissolved sulphate and rapid depletion of the sulphate pool in the presence of abundant organic matter allows bacterial methanogenic processes to dominate the earliest stages of diagenesis (Talbot & Kelts, 1990; Cerling, 1996). The grass-like Na-carbonate evaporites (trona + wegscheiderite) of the Fengcheng Formation, representative of primary chemical precipitates from lake waters (Yu *et al.*, 2018), show a slightly lower carbon isotopic range (+2.9 to +5.3‰) than organogenic dolomite (Fig. 9; Table S1), indicating that methanogenesis has not induced a large carbon isotopic fractionation between dolomite and dissolved inorganic carbon. This is because the vast inherent dissolved inorganic carbon pools of alkaline lakes made the carbon isotopic fractionation by metabolic activity, such as respiration, photosynthesis, organic matter oxidation or degradation, negligible and indiscernible (Benson *et al.*, 1991). Methanogenesis typically occurs via the reduction of CO_2 by H_2 or the fermentation of acetate or other organic substrates, the former process of which generally proceeds initially via reduction of CO_2 (or HCO_3^-) liberated by decarboxylation of organic matter during sulphate reduction. However, the absence of this CO_2 source in sulphate-poor porewaters of alkaline lakes means that fermentation provides the initial methanogenic pathway (Talbot & Kelts, 1990; Tosca & Wright, 2015). A remarkable increase of porewater dissolved CO_2 concentration, which is produced by methane formation via the fermentation pathway, has recently been detected in many modern alkaline lakes (Kuivila *et al.*, 1989; Cerling, 1996).

In lakes with negligible sulphate, methanogenic reactions during the early stages of diagenesis could result in locally fluctuating oxygen tensions, promoting the precipitation of zoned dolomite rhombs (Southgate *et al.*, 1989). This could well explain the zoned luminescence and fluorescence of isolated dispersed dolomite in the Fengcheng Formation, as well as its much larger crystal size (>20 μm) than those reported in other non-alkaline lake deposits (<10 μm). Large, isolated dolomite crystals (20 to 70 μm) are also the major dolomite type in the saline alkaline lacustrine Wilkins Peak Member of the Green River Formation, which are much larger in size than the dolomite crystals of the overlying meromictic brackish lacustrine Laney Member (5 to 10 μm) (Murphy *et al.*, 2014). Since most reported primary dolomite (Ca-rich dolomite or very high Mg-calcite) crystals, that generated in microbial mats or on Mg-clay mineral surfaces in environmental depositional settings (Casado *et al.*, 2014; Liu *et al.*, 2019; Wen *et al.*, 2020) occur at the nanometre scale (Sánchez-Román *et al.*, 2008), the large dolomite crystals of the Wilkins Peak Member and Fengcheng Formation were interpreted to have undergone overgrowth on tiny primary nuclei. The zoned dark red to olive green cathode-luminescence and zoned bright fluorescence suggest an anoxic, organic-rich environment for dolomite growth in the shallow subsurface, a specific subsurface milieu that could continue supplying Mg^{2+}, Ca^{2+} and CO_3^{2-}. The dissolution or transformation of Mg-clays and Mg-evaporites in the lake transitional sediments caused by methanogenesis and organic matter decay could provide Mg^{2+} ions for the continued growth of dolomite.

The organogenic dolomite formation driven by microbial methanogenesis in the saline alkaline lake of the Fengcheng Formation conforms to the 'fluctuation' model highlighted by Deelman (2011, 2021). The changing pH values from lake-water high level to porewater low level played an important, or even a key role in the stabilization of Mg by dolomite. The initial high pH levels facilitated dehydration of Mg^{2+}–H_2O complexes and promoted the formation of Mg-Na-carbonate evaporites (at high salinity values) and Mg-rich clays (at low salinity values) in water columns and near the water–sediment interface. The subsequent pH drop during organic matter degradation driven by bacterial methanogenesis caused the dissolution of Mg-Na-carbonate evaporites and Mg-rich clays, re-releasing Mg^{2+} ions and promoting dolomite nucleation and growth. Since methanogenesis zones are much larger in thickness than sulphate-reduction zones (Mazzullo, 2000), provided that organic matter is rich in sediments, the long-standing bacterial methanogenesis can not only promote dolomite nucleation, but also guarantee its long-lasting growth, resulting in the formation of much larger organogenic dolomite crystals than those in non-alkaline sedimentary systems. Because the impact of methanogenesis on pH is not as large as sulphate reduction and only half the amount of CO_2 is produced (Soetaert *et al.*, 2007), the methanogenesis-induced dissolution of Mg-rich clays and Mg-Na-carbonate evaporites was probably a gradual process and their supply of free Mg^{2+} ions for dolomite formation was

consequently also a slow process. In addition to the rarity of micritic calcium carbonate minerals due to phosphate inhibition in alkaline environments (Pietzsch *et al.*, 2022), the total amounts of dolomite crystals could not be very high, which can well explain why dolomite is commonly present in ancient alkaline saline lake deposits, but seldom exceeds over 50% (Boak & Poole, 2015; Guo *et al.*, 2021). In the competitive and organogenic model, the drop of porewater pH to below 8.5 driven by organic matter decay is the key for dolomite nucleation and growth. Although saline alkaline lake-central mudstones also contain abundant organic matter, the produced organic acids and CO_2 by microbial methanogenesis were not enough to dissolve the vast majority of Na-carbonate evaporites and to induce a detectable pH drop (Fig. 11). In the lake-marginal mudstones, preserved organic matter was limited, microbial methanogenesis was weak and effective pH drop could also not be achieved.

The competitive, organogenic dolomite formation model of the Fengcheng Formation suggests that the preferential uptake of Mg^{2+} ions during the authigenesis of eitelite, northupite or Mg-clays in the alkaline water column and near the water–sediment interface has greatly influenced dolomite formation, which should be considered as an important external barrier for low-T dolomite formation. The rarity of dolomite in the central deposits of alkaline saline lakes suggests that the promotion of highly alkaline conditions in low-T dolomite formation is conditional and restrained under most situations (Chase *et al.*, 2021), which prompts the authors to critically regard the high salinity and/or high alkalinity as favourable conditions for dolomite formation, and to revisit the 'Precambrian soda ocean' hypothesis (Kempe & Degens, 1985; Meister, 2013). The local distribution of dolomite in the organic-rich mudstones of the Fengcheng Formation highlights the important role of anaerobic degradation of organic matter in helping dolomite to procure Mg^{2+} from other Mg-rich evaporites and clays, not by enhancing pH and carbonate alkalinity as stressed in previous microbial dolomite models (Mazzullo, 2000; Roberts *et al.*, 2004; Sánchez-Román *et al.*, 2008, 2009b, 2011a), but by inducing the decrease of porewater pH (Cerling, 1996; Meister, 2013; Tosca & Wright, 2015; Wright & Barnett, 2015) and promoting the dissolution of Mg-Na-carbonates and Mg-clays. Since both the microbially-induced decrease and increase of solution pH could induce low-T dolomite formation under certain hydrochemical conditions, the fluctuations in pH might be the vital factor for dolomite formation.

CONCLUSIONS

High water alkalinity (pH > 9) is a commonly acknowledged condition conducive for low-temperature dolomite formation. This basin-wide survey of Mg-rich minerals in a Late Palaeozoic saline alkaline lake deposit displays a zoned distribution of Mg-rich minerals: eitelite and northupite in the lake-central zone, dolomite in the lake-transitional zone and Mg-clays (Mg-illite and clinochlore) in the lake-marginal zone, demonstrating a restricted environment for dolomite formation. This restriction collectively arises from the slow crystallization rates of dolomite due to its intrinsic kinetic inhibitor, the rarity of calcium carbonate precursors due to the enhanced phosphate inhibition and the concurrent increased activity of $SiO_{2(aq)}$ in highly alkaline conditions, creating an environment more favourable for the authigenesis of other Mg-rich minerals (northupite, eitelite or Mg-clays). Despite being under a competitive disadvantage for Mg^{2+}, primary dolomite could nucleate and grow progressively in Mg-evaporite-lean organic-rich sediments, where methanogenic anaerobic degradation of organic matter can produce organic acids and CO_2 to decrease porewater pH effectively, leading to the dissolution of Mg-clays and Na-Mg-carbonates, and the nucleation and long-lasting growth of dolomite. The effective pH decreases cannot be easily realized in lake-central mudstones due to the vast majority of pH-buffering Na-carbonate evaporites or in lake-marginal mudstones because of the rarity of organic matter and weak methanogenesis. The basin-wide investigation of Mg-mineral distribution reveals a previously unstressed external barrier for low-temperature dolomite formation and highlights the important role of organic matter degradation in helping dolomite to win the competition of Mg^{2+} from Na-Mg-carbonates (eitelite and northupite) and Mg-clays.

ACKNOWLEDGEMENTS

We would like to thank Dr Benjamin Tutolo and Dr Huifang Xu for their constructive reviews to improve this manuscript, and Dr Hilary Corlett

and Alexander Brasier for handling our manuscript. We acknowledge continuous support for core observation and sampling from the Xinjiang Oil Company of PetroChina. We thank Dr Javier García-Veigas in the CCiTUB of Universitat de Barcelona for his help in identifying saline minerals. This work is co-supported by National Natural Science Foundation of China (No. 42272117, 42002116). MSR acknowledges support from the Dutch Research Council (NWO) Project Nr.: OCENW.KLEIN.037.

DATA AVAILABILITY STATEMENT

Data sharing is not applicable to this article as no new data were created or analyzed in this study.

REFERENCES

Arad, A. and **Morton, W.H.** (1969) Mineral springs and saline lakes of the Western Rift Valley, Uganda. *Geochim. Cosmochim. Acta*, **33**, 1169–1181.

Azmy, K., **Lavoie, D.**, **Wang, Z.**, **Brand, U.**, **Al-Aasm, I.**, **Jackson, S.** and **Girard, I.** (2013) Magnesium-isotope and REE compositions of Lower Ordovician carbonates from Eastern Laurentia: implications for the origin of dolomites and limestones. *Chem. Geol.*, **356**, 64–75.

Baker, P.A. and **Burns, S.J.** (1985) Occurrence and formation of dolomite in organic-rich continental margin sediments. *Bull. Am. Assoc. Pet. Geol.*, **69**, 1917–1930.

Bao, Z., **Huang, K.**, **Huang, T.**, **Shen, B.**, **Zong, C.**, **Chen, K.** and **Yuan, H.** (2019) Precise magnesium isotope analyses of high-K and low-Mg rocks by MC-ICP-MS. *J. Anal. At. Spectrom*, **34**, 940–953.

Benson, L.V., **Meyers, P.A.** and **Spencer, R.J.** (1991) Change in the size of Walker Lake during the past 5000 years. *Palaeogeogr. Palaeoclimatol. Palaeoecol.*, **81**, 189–214.

Blättler, C.L., **Miller, N.R.** and **Higgins, J.A.** (2015) Mg and Ca isotope signatures of authigenic dolomite in siliceous deep-sea sediments. *Earth Planet. Sci. Lett.*, **419**, 32–42.

Blue, C.R. and **Dove, P.M.** (2015) Chemical controls on the magnesium content of amorphous calcium carbonate. *Geochim. Cosmochim. Acta*, **148**, 23–33.

Boak, J. and **Poole, S.** (2015) Mineralogy of the green river formation in the Piceance Creek basin, Colorado. In: *Stratigraphy and Paleolimnology of the Green River Formation, Western USA* (Eds Smith, M.E. and Carroll, A.R.), pp. 183–209. Springer Netherlands, Berlin.

Bourdon, B., **Tipper, E.T.**, **Fitoussi, C.** and **Stracke, A.** (2010) Chondritic Mg isotope composition of the Earth. *Geochim. Cosmochim. Acta*, **74**, 5069–5083.

Bowen, G.J., **Daniels, A.L.** and **Bowen, B.B.** (2008) Paleoenvironmental isotope geochemistry and paragenesis of lacustrine and palustrine carbonates, Flagstaff formation, Central Utah, U.S.A. *J. Sediment. Res.*, **78**, 162–174.

Bradley, W.H. and **Eugster, H.P.** (1969) Geochemistry and paleolimnology of the trona deposits and associated authigenic minerals of the Green River Formation of Wyoming. Professional Paper 496-B, 1–71.

Bristow, T.F., **Kennedy, M.J.**, **Morrison, K.D.** and **Mrofka, D.D.** (2012) The influence of authigenic clay formation on the mineralogy and stable isotopic record of lacustrine carbonates. *Geochim. Cosmochim. Acta*, **90**, 64–82.

del Buey, P. and **Sanz-Montero, M.E.** (2022) Biomineralization of ordered dolomite and magnesian calcite by the green alga Spirogyra. *Sedimentology*, **70**, 685–704.

del Buey, P., **Cabestrero, Ó.**, **Arroyo, X.** and **Sanz-Montero, M.E.** (2018) Microbially induced palygorskite-sepiolite authigenesis in modern hypersaline lakes (Central Spain). *Appl. Clay Sci.*, **160**, 9–21.

Calvo, J.P., **Jones, B.F.**, **Bustillo, M.**, **Fort, R.**, **Alonso Zarza, A.M.** and **Kendall, C.** (1995) Sedimentology and geochemistry of carbonates from lacustrine sequences in the Madrid Basin, central Spain. *Chem. Geol.*, **123**, 173–191.

Cao, J., **Xia, L.**, **Wang, T.**, **Zhi, D.**, **Tang, Y.** and **Li, W.** (2020) An alkaline lake in the Late Paleozoic Ice Age (LPIA): a review and new insights into paleoenvironment and petroleum geology. *Earth-Sci. Rev.*, **202**, 103091.

Carroll, A.R., **Yunhai, L.**, **Graham, S.A.**, **Xuchang, X.**, **Hendrix, M.S.**, **Jinchi, C.** and **McKnight, C.L.** (1990) Junggar basin, Northwest China: trapped Late Paleozoic ocean. *Tectonophysics*, **181**, 1–14.

Casado, A.I., **Alonso-Zarza, A.M.** and **La Iglesia, Á.** (2014) Morphology and origin of dolomite in paleosols and lacustrine sequences. Examples from the Miocene of the Madrid Basin. *Sed. Geol.*, **312**, 50–62.

Cerling, T.E. (1996) Pore water chemistry of an alkaline lake: Lake Turkana, Kenya. In: *The Limnology, Climatology and Paleoclimatology of the East African Lakes* (Eds Johnson, T.C. and Odada, E.O.), pp. 225–240. Gordon and Breach Publishers, Toronto, ON.

Chahi, A., **Duringer, P.**, **Ais, M.**, **Bouabdelli, M.** and **Fritz, F.G.-L.B.** (1999) Diagenetic transformation of dolomite into stevensite in lacustrine sediments from Jbel Rhassoul, Morocco. *J. Sediment. Res.*, **69**, 1123–1135.

Chase, J.E., **Arizaleta, M.L.** and **Tutolo, B.M.** (2021) A series of data-driven hypotheses for inferring biogeochemical conditions in alkaline lakes and their deposits based on the behavior of Mg and SiO_2. *Minerals*, **11**, 1–19.

Deelman, J.C. (2011) *Low-Temperature Formation of Dolomite and Magnesite (Version 2.3)*. Geology SeriesCompact Disc Publication, Eindhoven, The Netherlands.

Deelman, J.C. (2021) Magnesite, dolomite and carbonate groups. HAL Open Sci., [Research Report] (formerly) Technische Universiteit Eindhoven, 1–24.

Díaz-Hernández, J.L., **Sánchez-Navas, A.** and **Reyes, E.** (2013) Isotopic evidence for dolomite formation in soils. *Chem. Geol.*, **347**, 20–33.

Dyni, J.R. (1996) Sodium carbonate resources of the Green River Formation: Colorado, US Geological Survey. Open-File Report 96-729, 1–42.

Eugster, H.P. and **Surdam, R.C.** (1973) Depositional environment of the Green River Formation of Wyoming: a preliminary report. *Bull. Geol. Soc. Am.*, **84**, 1115–1120.

Fang, Y. and **Xu, H.** (2022) Dissolved silica-catalyzed disordered dolomite precipitation. *Am. Mineral.*, **107**, 443–452.

Fang, Y., **Hobbs, F.**, **Yang, Y.** and **Xu, H.** (2023) Dissolved silica-driven dolomite precipitation in the Great Salt Lake,

Utah, and its implication for dolomite formation environments. *Sedimentology*, **70**, 1328–1347.

Fantle, M.S. and **Higgins, J.** (2014) The effects of diagenesis and dolomitization on Ca and Mg isotopes in marine platform carbonates: Implications for the geochemical cycles of Ca and Mg. *Geochim. Cosmochim. Acta*, **142**, 458–481.

Fussmann, D., **Jean Elisabeth Von Hoyningen-Huene, A.**, **Reimer, A.**, **Schneider, D.**, **Babková, H.**, **Peticzka, R.**, **Maier, A.**, **Arp, G.**, **Daniel, R.** and **Meister, P.** (2020) Authigenic formation of Ca-Mg carbonates in the shallow alkaline Lake Neusiedl, Austria. *Biogeosciences*, **17**, 2085–2106.

Galy, A., **Bar-Matthews, M.**, **Halicz, L.** and **O'Nions, R.K.** (2002) Mg isotopic composition of carbonate: Insight from speleothem formation. *Earth Planet. Sci. Lett.*, **201**, 105–115.

Geske, A., **Zorlu, J.**, **Richter, D.K.**, **Buhl, D.**, **Niedermayr, A.** and **Immenhauser, A.** (2012) Impact of diagenesis and low grade metamorphosis on isotope (δ^{26}Mg, δ^{13}C, δ^{18}O and ^{87}Sr/^{86}Sr) and elemental (Ca, Mg, Mn, Fe and Sr) signatures of Triassic sabkha dolomites. *Chem. Geol.*, **332–333**, 45–64.

Guo, P., **Liu, C.**, **Wang, L.**, **Zhang, G.** and **Fu, X.** (2019) Mineralogy and organic geochemistry of the terrestrial lacustrine pre-salt sediments in the Qaidam Basin: implications for good source rock development. *Mar. Pet. Geol.*, **107**, 149–162.

Guo, P., **Wen, H.**, **Gibert, L.**, **Jin, J.**, **Wang, J.** and **Lei, H.** (2021) Deposition and diagenesis of the Early Permian volcanic-related alkaline playa-lake dolomitic shales, NW Junggar Basin, NW China. *Mar. Pet. Geol.*, **123**, 104780.

Hackley, P.C., **Fishman, N.**, **Wu, T.** and **Baugher, G.** (2016) Organic petrology and geochemistry of mudrocks from the lacustrine Lucaogou Formation, Santanghu Basin, northwest China: application to lake basin evolution. *Int. J. Coal Geol.*, **168**, 20–34.

Handler, M.R., **Baker, J.A.**, **Schiller, M.**, **Bennett, V.C.** and **Yaxley, G.M.** (2009) Magnesium stable isotope composition of Earth's upper mantle. *Earth Planet. Sci. Lett.*, **282**, 306–313.

Hay, R.L. and **Guldman, S.G.** (1987) Diagenetic alteration of Silicic Ash in Searles Lake, California. *Clay Clay Mineral.*, **35**, 449–457.

Hay, R.L., **Guldman, S.G.**, **Matthews, J.C.**, **Lander, R.H.**, **Duffin, M.E.** and **Kyser, T.K.** (1991) Clay mineral diagenesis in core KM-3 of Searles Lake, California. *Clay Clay Mineral.*, **39**, 84–96.

Higgins, J.A. and **Schrag, D.P.** (2010a) Constraining magnesium cycling in marine sediments using magnesium isotopes. *Geochim. Cosmochim. Acta*, **74**, 5039–5053.

Higgins, J.A. and **Schrag, D.P.** (2010b) The Mg isotopic composition of Cenozoic seawater - evidence for a link between Mg-clays, seawater Mg/Ca, and climate. *Earth Planet. Sci. Lett.*, **416**, 73–81.

Hobbs, F.W.C. and **Xu, H.** (2020) Magnesite formation through temperature and pH cycling as a proxy for lagoon and playa paleoenvironments. *Geochim. Cosmochim. Acta*, **269**, 101–116.

Huang, K.J., **Teng, F.Z.**, **Elsenouy, A.**, **Li, W.Y.** and **Bao, Z.Y.** (2013) Magnesium isotopic variations in loess: origins and implications. *Earth Planet. Sci. Lett.*, **374**, 60–70.

Huang, K.J., **Shen, B.**, **Lang, X.G.**, **Tang, W.B.**, **Peng, Y.**, **Ke, S.**, **Kaufman, A.J.**, **Ma, H.R.** and **Li, F.B.** (2015) Magnesium isotopic compositions of the Mesoproterozoic dolostones: implications for Mg isotopic systematics of marine carbonates. *Geochim. Cosmochim. Acta*, **164**, 333–351.

Immenhauser, A., **Buhl, D.**, **Richter, D.**, **Niedermayr, A.**, **Riechelmann, D.**, **Dietzel, M.** and **Schulte, U.** (2010) Magnesium-isotope fractionation during low-Mg calcite precipitation in a limestone cave – field study and experiments. *Geochim. Cosmochim. Acta*, **74**, 4346–4364.

Kaczmarek, S.E., **Gregg, J.M.**, **Bish, D.L.**, **Machel, H.G.** and **Fouke, B.W.** (2017) Dolomite, very high-magnesium calcite, and microbes—implications for the microbial model of dolomitization. In: *Characterization and Modeling of Carbonates–Mountjoy Symposium 1* (Eds MacNeil, A.J., Lonnee, J. and Wood, R.), *SEPM (Society for Sedimentary Geology)*, **109**, 1–14. SEPM Special Publications, Tulsa, OK.

Kasemann, S.A., **Pogge von Strandmann, P.A.E.**, **Prave, A.R.**, **Fallick, A.E.**, **Elliott, T.** and **Hoffmann, K.H.** (2014) Continental weathering following a Cryogenian glaciation: evidence from calcium and magnesium isotopes. *Earth Planet. Sci. Lett.*, **396**, 66–77.

Kempe, S. and **Degens, E.T.** (1985) An early soda ocean? *Chem. Geol.*, **53**, 95–108.

Kilham, P. and **Melack, J.M.** (1972) Primary northupite deposition in Lake Mahega, Uganda. *Science*, **238**, 123.

Kuivila, K.M., **Murray, J.W.**, **Devol, A.H.** and **Novelli, P.C.** (1989) Methane production, sulfate reduction and competition for substrates in the sediments of Lake Washington. *Geochim. Cosmochim. Acta*, **53**, 409–416.

Last, W.M. (1990) Lacustrine dolomite-an overview of modern, Holocene, and Pleistocene occurrences. *Earth Sci. Rev.*, **27**, 221–263.

Last, F.M., **Last, W.M.** and **Halden, N.M.** (2012) Modern and late Holocene dolomite formation: Manito Lake, Saskatchewan, Canada. *Sed. Geol.*, **281**, 222–237.

Lavoie, D., **Jackson, S.** and **Girard, I.** (2014) Magnesium isotopes in high-temperature saddle dolomite cements in the lower Paleozoic of Canada. *Sed. Geol.*, **305**, 58–68.

Leguey, S., **De León, D.R.**, **Ruiz, A.I.** and **Cuevas, J.** (2010) The role of biomineralization in the origin of sepiolite and dolomite. *Am. J. Sci.*, **310**, 165–193.

Li, W.Y., **Teng, F.Z.**, **Ke, S.**, **Rudnick, R.L.**, **Gao, S.**, **Wu, F.Y.** and **Chappell, B.W.** (2010) Heterogeneous magnesium isotopic composition of the upper continental crust. *Geochim. Cosmochim. Acta*, **74**, 6867–6884.

Li, F.B., **Teng, F.Z.**, **Chen, J.T.**, **Huang, K.J.**, **Wang, S.J.**, **Lang, X.G.**, **Ma, H.R.**, **Peng, Y.B.** and **Shen, B.** (2016) Constraining ribbon rock dolomitization by Mg isotopes: implications for the "dolomite problem". *Chem. Geol.*, **445**, 208–220.

Li, M., **Chen, Z.**, **Cao, T.**, **Ma, X.**, **Liu, X.**, **Li, Z.**, **Jiang, Q.** and **Wu, S.** (2018) Expelled oils and their impacts on Rock-Eval data interpretation, Eocene Qianjiang Formation in Jianghan Basin, China. *Int. J. Coal Geol.*, **191**, 37–48.

Liu, C., **Wang, Z.**, **Raub, T.D.**, **Macdonald, F.A.** and **Evans, D.A.D.** (2014) Neoproterozoic cap-dolostone deposition in stratified glacial meltwater plume. *Earth Planet. Sci. Lett.*, **404**, 22–32.

Liu, D., **Xu, Y.**, **Papineau, D.**, **Yu, N.**, **Fan, Q.**, **Qiu, X.** and **Wang, H.** (2019) Experimental evidence for abiotic formation of low-temperature proto-dolomite facilitated by clay minerals. *Geochim. Cosmochim. Acta*, **247**, 83–95.

Lowenstein, T.K., **Jagniecki, E.A.**, **Carroll, A.R.**, **Smith, M.E.**, **Renaut, R.W.** and **Owen, R.B.** (2017) The Green River salt mystery: what was the source of the hyperalkaline lake waters? *Earth-Sci. Rev.*, **173**, 295–306.

Mazzullo, S.J. (2000) Organogenic dolomitization in peritidal to deep-sea sediments. *J. Sed. Res.*, **70**, 10–23.

McCormack, J., **Bontognali, T.R.R.**, **Immenhauser, A.** and **Kwiecien, O.** (2018) Controls on cyclic formation of quaternary early diagenetic dolomite. *Geophys. Res. Lett.*, **45**, 3625–3634.

Mees, F., **Verschuren, D.**, **Nijs, R.** and **Dumont, H.** (1991) Holocene evolution of the crater lake at Malha, Northwest Sudan. *J. Paleolimnol.*, **5**, 227–253.

Meister, P. (2013) Two opposing effects of sulfate reduction on carbonate precipitation in normal marine, hypersaline, and alkaline environments. *Geology*, **41**, 499–502.

Meister, P. and **Frisia, S.** (2019) Dolomite formation by nanocrystal aggregation in the Dolomite Principale of the Brenta Dolomites (Northern Italy). *Riv. Ital. Paleontol. Stratigr.*, **125**, 183–196.

Meister, P., **Reyes, C.**, **Beaumont, W.**, **Rincon, M.**, **Collins, L.**, **Berelson, W.**, **Stott, L.**, **Corsetti, F.** and **Nealson, K.H.** (2011) Calcium and magnesium-limited dolomite precipitation at Deep Springs Lake, California. *Sedimentology*, **58**, 1810–1830.

Mercedes-Martín, R., **Ayora, C.**, **Tritlla, J.** and **Sánchez-Román, M.** (2019) The hydrochemical evolution of alkaline volcanic lakes: a model to understand the Cretaceous Presalt mineral assemblages. *Earth-Sci. Rev.*, **198**, 102938.

Milesi, V.P., **Jézéquel, D.**, **Debure, M.**, **Cadeau, P.**, **Guyot, F.**, **Sarazin, G.**, **Claret, F.**, **Vennin, E.**, **Chaduteau, C.**, **Virgone, A.**, **Gaucher, E.C.** and **Ader, M.** (2019) Formation of magnesium-smectite during lacustrine carbonates early diagenesis: study case of the volcanic crater lake Dziani Dzaha (Mayotte – Indian Ocean). *Sedimentology*, **66**, 983–1001.

Milton, C. (1971) Authigenic minerals of the Green River Formation. *Rocky Mt. Geol.*, **10**, 57–63.

Murphy, J.T., **Lowenstein, T.K.** and **Pietras, J.T.** (2014) Preservation of primary lake signatures in alkaline earth carbonates of the Eocene Green River Wilkins Peak-Laney Member transition zone. *Sed. Geol.*, **314**, 75–91.

Olson, K.J. and **Lowenstein, T.K.** (2021) Searles Lake evaporite sequences: indicators of late Pleistocene/Holocene lake temperatures, brine evolution, and pCO_2. *GSA Bull.*, **133**, 2319–2334.

Ortí, F., **Rosell, L.**, **Garcia, J.** and **Helvaci, C.** (2016) Sulfate-Borate association (Glauberite – Probertite) in the Emet Basin: Implications for evaporite Sedimentology Middle Miocene, Turkey. *J. Sediment. Res.*, **86**, 448–475.

Peng, Y., **Hen, B.**, **Lang, X.G.**, **Huang, K.J.**, **Chen, J.T.**, **Yan, Z.**, **Tang, W.B.**, **Ke, S.**, **Ma, H.R.** and **Li, F.B.** (2016) Constraining dolomitization by Mg isotopes: a case study from partially dolomitized limestones of the Middle Cambrian Xuzhuang Formation, North China. *Geochem. Geophys. Geosyst.*, **17**, 1109–1129.

Perri, E., **Tucker, M.E.**, **Słowakiewicz, M.**, **Whitaker, F.**, **Bowen, L.** and **Perrotta, I.D.** (2018) Carbonate and silicate biomineralization in a hypersaline microbial mat (Mesaieed sabkha, Qatar): roles of bacteria, extracellular polymeric substances and viruses. *Sedimentology*, **65**, 1213–1245.

Peterson, M.N.A., **Bien, G.S.** and **Berner, R.A.** (1963) Radiocarbon studies of recent dolomite from Deep Springs Lake, California. *J. Geophys. Res.*, **68**, 6493–6505.

Petrash, D.A., **Gueneli, N.**, **Brocks, J.J.**, **Méndez-Dot, J.A.**, **González-Arismendi, G.**, **Poulton, S.W.** and **Konhauser, K.O.** (2016) Black shale deposition and early diagenetic dolomite cementation during Oceanic Anoxic Event 1: the mid-Cretaceous Maracaibo Platform, Northwestern South America. *Am. J. Sci.*, **316**, 669–711.

Pietzsch, R., **Tosca, N.J.**, **Gomes, J.P.**, **Roest-Ellis, S.**, **Sartorato, A.C.L.** and **Tonietto, S.N.** (2022) The role of phosphate on non-skeletal carbonate production in a Cretaceous alkaline lake. *Geochim. Cosmochim. Acta*, **317**, 365–394.

Pimentel, C. and **Pina, C.M.** (2016) Reaction pathways towards the formation of dolomite-analogues at ambient conditions. *Geochim. Cosmochim. Acta*, **178**, 259–267.

Pogge von Strandmann, P.A.E., **Opfergelt, S.**, **Lai, Y.J.**, **Sigfússon, B.**, **Gislason, S.R.** and **Burton, K.W.** (2012) Lithium, magnesium and silicon isotope behaviour accompanying weathering in a basaltic soil and pore water profile in Iceland. *Earth Planet. Sci. Lett.*, **339–340**, 11–23.

Pokrovsky, B.G., **Mavromatis, V.** and **Pokrovsky, O.S.** (2011) Co-variation of Mg and C isotopes in late Precambrian carbonates of the Siberian Platform: a new tool for tracing the change in weathering regime? *Chem. Geol.*, **290**, 67–74.

Power, I.M., **Harrison, A.L.**, **Dipple, G.M.**, **Wilson, S.A.**, **Barker, S.L.L.** and **Fallon, S.J.** (2019) Magnesite formation in playa environments near Atlin, British Columbia, Canada. *Geochim. Cosmochim. Acta*, **255**, 1–24.

Pozo, M. and **Calvo, J.** (2018) An overview of authigenic magnesian clays. *Minerals*, **8**, 520.

Raudsepp, M.J., **Wilson, S.A.**, **Morgan, B.**, **Patel, A.**, **Johnston, S.G.**, **Gagen, E.J.** and **Fallon, S.J.** (2022) Non-classical crystallization of very high magnesium calcite and magnesite in the Coorong Lakes, Australia. *Sedimentology*, **69**, 2246–2266.

Roberts, J.A., **Bennet, P.C.**, **Gonzalez, L.A.**, **Macpherson, G.L.** and **Milliken, K.L.** (2004) Microbial precipitation of dolomite in methanogenic groundwater. *Geology*, **32**, 277–280.

Ryan, B.H., **Kaczmarek, S.E.** and **Rivers, J.M.** (2019) Dolomite dissolution: an alternative diagenetic pathway for the formation of palygorskite clay. *Sedimentology*, **66**, 1803–1824.

Sánchez-Román, M., **Vasconcelos, C.**, **Schmid, T.**, **Dittrich, M.**, **McKenzie, J.A.**, **Zenobi, R.** and **Rivadeneyra, M.A.** (2008) Aerobic microbial dolomite at the nanometer scale: implications for the geologic record. *Geology*, **36**, 879–882.

Sánchez-Román, M., **McKenzie, J.A.**, **de Luca Rebello Wagener, A.**, **Rivadeneyra, M.A.** and **Vasconcelos, C.** (2009a) Presence of sulfate does not inhibit low-temperature dolomite precipitation. *Earth Planet. Sci. Lett.*, **285**, 131–139.

Sánchez-Román, M., **Vasconcelos, C.**, **Warthmann, R.**, **Rivadeneyra, M.** and **McKenzie, J.A.** (2009b) Microbial dolomite precipitation under aerobic conditions: results from Brejo do Espinho Lagoon (Brazil) and culture experiments. *Int. Assoc. Sedimentol. Spec. Publ.*, **41**, 167–178.

Sánchez-Román, M., **McKenzie, J.A.**, **de Luca Rebello Wagener, A.**, **Romanek, C.S.**, **Sánchez-Navas, A.** and **Vasconcelos, C.** (2011a) Experimentally determined biomediated Sr partition coefficient for dolomite: significance and implication for natural dolomite. *Geochim. Cosmochim. Acta*, **75**, 887–904.

Sánchez-Román, M., **Romanek, C.S.**, **Fernández-Remolar, D.C.**, **Sánchez-Navas, A.**, **McKenzie, J.A.**, **Pibernat, R.A.** and **Vasconcelos, C.** (2011b) Aerobic biomineralization of Mg-rich carbonates: implications for natural environments. *Chem. Geol.*, **281**, 143–150.

Sanz-Montero, M.E., **Rodriguez-Aranda, J.P.** and **Calvo, J.P.** (2006) Mediation of endoevaporitic microbial communities in early replacement of gypsum by dolomite: a case study from Miocene Lake deposits of the Madrid Basin, Spain. *J. Sed. Res.*, **76**, 1257–1266.

Sanz-Montero, M.E., **Rodríguez-Aranda, J.P.** and **García Del Cura, M.A.A.** (2008) Dolomite-silica stromatolites in Miocene lacustrine deposits from the Duero Basin, Spain: the role of organotemplates in the precipitation of dolomite. *Sedimentology*, **55**, 729–750.

Shen, Z., **Liu, Y.**, **Brown, P.E.**, **Szlufarska, I.** and **Xu, H.** (2014) Modeling the effect of dissolved hydrogen sulfide on Mg^{2+}-water complex on dolomite {104} surfaces. *J. Phys. Chem. C*, **118**, 15716–15722.

Shirokova, L.S., **Mavromatis, V.**, **Bundeleva, I.** and **Pokrovsky, O.S.** (2011) Can Mg isotopes be used to trace cyanobacteria-mediated magnesium carbonate precipitation in alkaline lakes? *Biogeosci. Discuss.*, **8**, 6473–6517.

Singer, A. and **Stoffers, P.** (1980) Clay mineral diagenesis in two East African lake sediments. *Clay Miner.*, **15**, 291–307.

Slaughter, M. and **Hill, R.J.** (1991) The influence of organic matter in organogenic dolomitization. *J. Sediment. Petrol.*, **61**, 296–303.

Smith, G.I. and **Stuiver, M.** (1979) *Subsurface Stratigraphy and Geochemistry of Late Quaternary Evaporites, Searles Lake, California*, pp. 1–118. United States Government Printing Office, Washington, DC.

Soetaert, K., **Hofmann, A.F.**, **Middelburg, J.J.**, **Meysman, F.J.R.** and **Greenwood, J.** (2007) The effect of biogeochemical processes on pH. *Mar. Chem.*, **105**, 30–51.

Southgate, P.N., **Lambert, I.B.**, **Donnelly, T.H.**, **Henry, R.**, **Etminan, H.** and **Weste, G.** (1989) Depositional environments and diagenesis in Lake Parakeelya: a Cambrian alkaline playa from the Officer Basin, South Australia. *Sedimentology*, **36**, 1091–1112.

Surdam, R.C. and **Parker, R.D.** (1972) Authigenic aluminosilicate minerals in the tuffaceous rocks of the Green River Formation, Wyoming. *Geol. Soc. Am. Bull.*, **83**, 2397–2418.

Talbot, M.R. and **Kelts, K.** (1990) Paleolimnological signatures from carbon and oxygen isotopic ratios in carbonates from organic carbon-rich lacustrine sediments. In: *Lacustrine Basin Exploration – Case Studies and Modern Analogs* (Ed Katz, B.J.), *Am. Assoc. Pet. Geol., Mem.*, **50**, 99–112. The American Association of Petroleum Geologists, Tulsa, OK.

Teng, F.Z., **Li, W.Y.**, **Ke, S.**, **Marty, B.**, **Dauphas, N.**, **Huang, S.**, **Wu, F.Y.** and **Pourmand, A.** (2010a) Magnesium isotopic composition of the Earth and chondrites. *Geochim. Cosmochim. Acta*, **74**, 4150–4166.

Teng, F.Z., **Li, W.Y.**, **Rudnick, R.L.** and **Gardner, L.R.** (2010b) Contrasting lithium and magnesium isotope fractionation during continental weathering. *Earth Planet. Sci. Lett.*, **300**, 63–71.

Tipper, E.T., **Galy, A.**, **Gaillardet, J.**, **Bickle, M.J.**, **Elderfield, H.** and **Carder, E.A.** (2006) The magnesium isotope budget of the modern ocean: constraints from riverine magnesium isotope ratios. *Earth Planet. Sci. Lett.*, **250**, 241–253.

Tipper, E.T., **Gaillardet, J.**, **Louvat, P.**, **Capmas, F.** and **White, A.F.** (2010) Mg isotope constraints on soil pore-fluid chemistry: evidence from Santa Cruz, California. *Geochim. Cosmochim. Acta*, **74**, 3883–3896.

Tosca, N.J. and **Wright, V.P.** (2015) Diagenetic pathways linked to labile Mg-clays in lacustrine carbonate reservoirs: a model for the origin of secondary porosity in the Cretaceous pre-salt Barra Velha Formation, offshore Brazil. *Geol. Soc. London Spec. Publ.*, **435**, 33–46.

Tutolo, B.M. and **Tosca, N.J.** (2018) Experimental examination of the Mg-silicate-carbonate system at ambient temperature: implications for alkaline chemical sedimentation and lacustrine carbonate formation. *Geochim. Cosmochim. Acta*, **225**, 80–101.

Vandeginste, V., **Snell, O.**, **Hall, M.R.**, **Steer, E.** and **Vandeginste, A.** (2019) Acceleration of dolomitization by zinc in saline waters. *Nat. Commun.*, **10**, 4–11.

Vasconcelos, C. and **McKenzie, J.A.** (1997) Microbial mediation of modern dolomite precipitation and diagenesis under anoxic conditions (Lagoa Vermelha, Rio De Janeiro, Brazil). *J. Sediment. Res.*, **67**, 378–390.

Wen, H.G., **Zheng, R.C.**, **Qing, H.**, **Fan, M.T.**, **Li, Y.A.** and **Gong, B.S.** (2013) Primary dolostone related to the Cretaceous lacustrine hydrothermal sedimentation in Qingxi sag, Jiuquan Basin on the northern Tibetan Plateau. *Sci. China Earth Sci.*, **56**, 2080–2093.

Wen, Y., **Sánchez-Román, M.**, **Li, Y.**, **Wang, C.**, **Han, Z.**, **Zhang, L.** and **Gao, Y.** (2020) Nucleation and stabilization of Eocene dolomite in evaporative lacustrine deposits from central Tibetan plateau. *Sedimentology*, **67**, 3333–3354.

Wimpenny, J., **Yin, Q.Z.**, **Tollstrup, D.**, **Xie, L.W.** and **Sun, J.** (2014) Using Mg isotope ratios to trace Cenozoic weathering changes: a case study from the Chinese Loess Plateau. *Chem. Geol.*, **376**, 31–43.

Wolfbauer, C.A. and **Surdam, R.C.** (1974) Origin of nonmarine dolomite in Eocene Lake Gosiute, Green River Basin, Wyoming. *Bull. Geol. Soc. Am.*, **85**, 1733–1740.

Wright, V.P. and **Barnett, A.J.** (2015) An abiotic model for the development of textures in some South Atlantic early Cretaceous lacustrine carbonates. *Geol. Soc. London Spec. Publ.*, **418**, 209–219.

Wright, D.T. and **Wacey, D.** (2005) Precipitation of dolomite using sulphate-reducing bacteria from the Coorong Region, South Australia: significance and implications. *Sedimentology*, **52**, 987–1008.

Xu, J., **Yan, C.**, **Zhang, F.**, **Konishi, H.**, **Xu, H.** and **Teng, H.H.** (2013) Testing the cation-hydration effect on the crystallization of Ca-Mg-CO_3 systems. *Proc. Natl Acad. Sci. USA*, **110**, 17750–17755.

Yang, Z., **Zhong, D.**, **Whitaker, F.**, **Lu, Z.**, **Zhang, S.**, **Tang, Z.**, **Liu, R.** and **Li, Z.** (2020) Syn-sedimentary hydrothermal dolomites in a lacustrine rift basin: petrographic and geochemical evidence from the lower Cretaceous Erlian Basin, Northern China. *Sedimentology*, **67**, 305–329.

Yao, G., **Li, L.**, **Cai, M.** and **Liu, Y.** (2017) Mechanisms of salinization in a middle Eocene lake in the Tanggu area of the Huanghua Depression. *Mar. Pet. Geol.*, **86**, 155–167.

Yu, K., **Cao, Y.**, **Qiu, L.**, **Sun, P.**, **Jia, X.** and **Wan, M.** (2018) Geochemical characteristics and origin of sodium carbonates in a closed alkaline basin: the Lower Permian Fengcheng Formation in the Mahu Sag, Northwestern Junggar Basin, China. *Palaeogeogr. Palaeoclimatol. Palaeoecol.*, **511**, 506–531.

Yu, K., **Cao, Y.**, **Qiu, L.** and **Sun, P.** (2019) Depositional environments in an arid, closed basin and their implications for oil and gas exploration: the lower Permian Fengcheng Formation in the Junggar Basin, China. *Am. Assoc. Pet. Geol. Bull.*, **103**, 2073–2115.

Zhang, F., **Xu, H.**, **Konishi, H.**, **Kemp, J.M.**, **Roden, E.E.** and **Shen, Z.** (2012) Dissolved sulfide-catalyzed precipitation

of disordered dolomite: implications for the formation mechanism of sedimentary dolomite. *Geochim. Cosmochim. Acta*, **97**, 148–165.

Zhou, S., **Wang, Y.** and **Teng, H.** (2021) Relative contributions of mg hydration and molecular structural restraints to the barrier of dolomite crystallization: a comparison of aqueous and non-aqueous crystallization in $(BaMg)CO_3$ and $(CaMg)CO_3$ systems. *Minerals*, **11**, 1214.

Zhu, S., **Qin, Y.**, **Liu, X.**, **Wei, C.**, **Zhu, X.** and **Zhang, W.** (2017) Origin of dolomitic rocks in the lower Permian Fengcheng formation, Junggar Basin, China: evidence from petrology and geochemistry. *Mineral. Petrol.*, **111**, 267–282.

Manuscript received 18 March 2023; revision accepted 19 June 2023

Supporting Information

Additional information may be found in the online version of this article:

Table S1. Stable isotope data of carbon and oxygen of different carbonate minerals in the Fengcheng Formation.

Table S2. Mineral compositions and Mg isotopes of the saline alkaline lake deposit in the Mahu Sag of the Junggar Basin.